

**Grapevine yield estimation using image analysis
for the variety Syrah**

Giuseppe Samà

Dissertation to obtain a Master's Degree in

Bologna Master Degree in Engenharia de Viticultura e Enologia

Supervisor: Carlos Manuel Antunes Lopes

Supervisor: Vittorino Novello

Jury:

President:

PhD Joaquim Miguel Rangel da Cunha Costa, Assistant Professor at Instituto Superior de Agronomia, Universidade de Lisboa.

Members:

PhD Carlos Manuel Antunes Lopes, Associate Professor at Instituto Superior de Agronomia, Universidade de Lisboa

PhD Ricardo Nuno da Fonseca Garcia Pereira Braga, Assistant Professor at Instituto Superior de Agronomia, Universidade de Lisboa

To my Family....

ACNOWLEDGEMENT

I wish first like to thank my thesis advisor Professor Carlos Lopes for the help provided to me in this period and for his availability and patience.

I should to thank at Goncalo Vitorino for the availability and help during all the work.

I would like to acknowledge Professor Vittorino Novello for all the availability to me and to be my Italian supervisor.

Thank at all the group of viticulture for working together and helping each other.

Thank at all my family for the support, especially my mother and my father who have always believed in me, giving courage in my studies in every situation.

I would like to thank all my friends, colleagues and all the people framed during all the study for the continuous encouragement and the permanence in Lisbon.

A special thank at my fantastic flatmates, because whit theme I shared one of the most beautiful and unforgettable periods of my life.

Thanks at all...

Giuseppe Samà

ABSTRACT

Yield estimation in recent years is identified as one of more important topics in viticulture because it can lead to more efficiently managed vineyards producing wines of highly quality. Recently, to improve the efficiency of yield estimation, image analysis is becoming an important tool to collect detailed information from the vines regarding the yield. New technologies were developed for yield estimation using a new ground platform, such as VINBOT, using image analysis. This work was done in a vineyard of the “*Instituto Superior de Agronomia*”, with the aim to estimate the final yield, during the growing cycle 2019 of the variety “Syrah”, using images collected by the VINBOT robot. The images were captured with the RGB-D camera placed on the VINBOT robot in the vineyard and in addition, we obtained laboratory images using an RGB-D manual camera. In this work, the correlation of yield components between ground truth data and images data was evaluated. In addition, it was evaluate the projected bunches area in the images and the percentage of visible bunches not occluded by leaves and by other bunches. It was found a growth factor of bunches on the periods from pea-size to harvest. The efficacy to estimate bunch weight from the projected area was higher at maturation. The relationship between canopy porosity and exposed bunches showed for all the stages high and significant R^2 indicating that we can use it to estimate bunches covered by leaves through image analysis. The percentage of visible bunches without the leaves occlusion and bunch occlusion was 29% at pea-size, 21% at veraison and 45% at maturation. It was estimated the final yield at pea-size, with an MA%E of 54%, at veraison and maturation were observed values of MA%E of 7% and 5%, respectively. Our results enable to conclude that the image analysis is an alternative to the traditional way to estimate the yield.

Key words: Yield estimation, precision viticulture, Vinbot, image analysis, Syrah

RESUMO

A estimativa do rendimento em viticultura nos últimos é identificada como um dos temas mais importantes porque pode levar a vinhas mais eficientemente geridas produzindo vinhos de melhor qualidade. Para melhorar a eficiência da estimativa do rendimento, a análise de imagem é uma ferramenta importante para colher informações detalhadas das vinhas. Novas tecnologias são desenvolvidas para estimar o rendimento usando uma nova plataforma terrestre, como o robô VINBOT que utiliza análise de imagem. Este trabalho foi realizado numa vinha do “Instituto Superior de Agronomia”, para estimar o rendimento final, durante o ciclo biológico 2019 na casta “Syrah”, com base em imagens colhidas pelo robô VINBOT. As imagens foram capturadas com a câmara RGB-D colocada no robô VINBOT na vinha e, além disso, obtivemos imagens de laboratório usando uma câmara manual RGB-D. Neste trabalho foi avaliada a correlação das componentes de rendimento observadas no campo e os dados obtidos nas imagens. Para além disso, foi avaliada a área projectada dos cachos nas imagens, a percentagem de cachos visíveis sem a oclusão por folhas e por outros cachos. Foi encontrado um fator de crescimento de cachos. A eficácia para estimar o peso de cacho com base na área projectada foi elevada na maturação. A relação entre porosidade da sebee a percentagem de cachos expostos mostrou para todos os estados fenológicos valores elevados e significativos de R^2 indicando que podemos usar a porosidade para estimar cachos cobertos por folhas através da análise de imagem. A percentagem de cachos visíveis sem oclusão das folhas e cachos foi de 29% ao bago de ervilha, 21% ao pintor e 45% à maturação. Estimou-se o rendimento final obtido ao bago de ervilha, com MA%E de 54%, enquanto que ao pintor e à maturação foram observados valores de MA%E de 7% e 5%, respectivamente. A partir do resultado deste trabalho, é possível concluir que a análise de imagens é uma alternativa aos métodos tradicionais de estimar o rendimento.

Palavras-chave: Estimativa do rendimento, viticultura de precisão, Vinbot, análise de imagem, Syrah

RESUMO ALARGADO

A estimativa do rendimento nos últimos anos é identificada como um dos temas mais importantes na viticultura. Uma previsão precisa do rendimento poderá conduzir a uma gestão mais eficiente das vinhas para produção de vinhos de melhor qualidade. Uma boa previsão de rendimento prepara os produtores para decidir as necessidades de monda de cachos, para organizar a colheita, para organizar o espaço dentro e fora da adega, para gerir o mercado de uva e vinho, para programar o investimento e desenvolver estratégias de marketing. O rendimento é determinado pelos componentes de rendimento, como o número de videiras, o número de cachos, o número de bagos e o peso do bago e cacho. Normalmente, a previsão de rendimento é realizada usando valores históricos e padrões climáticos, juntamente com medições e monitorização de videiras numa determinada amostra de videiras. Muitas vezes estas medições não fornecem uma estimativa precisa do rendimento final. Recentemente, estão a ser investigados métodos de análise de imagem não invasivos que permitem a recolha eficiente de informações detalhadas sobre o rendimento das vinhas. A análise de imagem pode permitir a criação de sistemas capazes de estimar o rendimento sem necessidade de contato e de forma rápida e precisa. Este trabalho foi realizado numa vinha do “Instituto Superior de Agronomia”, para estimar o rendimento final, durante o ciclo de crescimento 2019 na casta ‘Syrah’, usando imagens colhidas pelo robô VINBOT. As imagens foram capturadas com a câmara RGB-D colocada no robô VINBOT na vinha e, além disso, obtivemos imagens de laboratório usando uma câmara manual RGB-D. Estas imagens foram analisadas para avaliar a relação entre os dados reais do campo e as imagens. As imagens foram utilizadas para desenvolver modelos para estimar os cachos não visíveis, porque obstruídos por folhas e outros cachos, e foi avaliada a área projectada dos cachos nas imagens. As imagens foram analisadas utilizando o software “imageJ”. Foi encontrado um fator de crescimento de cachos. O desenvolvimento dos bagos apresentou um fator de crescimento do bago de ervilha ao pintor de 2.5, e entre o pintor e a vindima de 1.09. A eficácia para estimar o peso do cacho através da área projectada foi elevada na maturação ($R^2=0.90$), enquanto no bago de ervilha a regressão apresentou um $R^2=0.59$ e ao pintor um $R^2=0.61$. A análise de regressão linear entre os cachos expostos e a porosidade da sebe apresentou um $R^2=0.85$ ao bago da ervilha, $R^2=0.91$ ao pintor e $R^2=0.76$ na maturação. A percentagem de cachos visíveis sem oclusão das folhas e oclusão do cacho foi de 29% ao bago de ervilha, 21% ao pintor e 45% à maturação. Para estimar o rendimento, do bago de ervilha à maturação, adicionando os modelos desenvolvidos, e utilizando a média de oclusão por cachos, e utilizando os fatores de crescimento foi possível estimar o rendimento final. Foi obtida um rendimento final no bago da ervilha, com um MA%E de 54%, enquanto ao pintor e à maturação foram observados

valores de MA%E de 7% e 5%, respectivamente. A partir do resultado deste trabalho, é possível concluir que a análise de imagens é uma alternativa aos métodos tradicionais de estimar o rendimento.

Palavras-chave: Estimativa do rendimento, viticultura de precisão, Vinbot, análise de imagem, Syrah

INDEX

- 1. INTRODUCTION..... 1
 - Aims of the work 2
- 2. LITERATURE REVIEW 3
 - 2.1 Precision viticulture..... 3
 - 2.2 Monitoring technologies 3
 - 2.2.1 Sensing platforms..... 3
 - 2.3 Remote sensing 4
 - 2.4 Proximal sensing 5
 - 2.5 Robotic platforms..... 6
 - 2.6 Image analysis as a precision viticulture tool..... 7
 - 2.6.1 Vegetation indexes..... 7
 - 2.6.2 Colour space..... 9
 - 2.7 Yield estimation 10
 - 2.7.1 Estimation method..... 10
 - 2.7.2 Image analysis 14
 - 2.8 Vinbot 20
- 3. MATERIALS AND METHODS..... 21
 - 3.1 Localization experiment 21
 - 3.2 Vinbot 23
 - 3.3 Cultural Practices..... 24
 - 3.4 Experiment design 24
 - 3.5 Methodologies 26
 - 3.5.1 Analysis of yield components 26
 - 3.5.2 Projected area of bunch and bunch weight..... 27
 - 3.5.3 Model for bunch estimation covered by leaves 28
 - 3.5.4 Model of bunch occlusion by bunch..... 28
 - 3.5.5 Berry and bunch growth factor..... 30
- 4. RESULTS AND DISCUSSIONS 31
 - 4.1 Analysis of yield components..... 31
 - 4.2 Projected area of bunch and weight..... 34
 - 4.3 Model for bunch estimation covered by leaves..... 36
 - 4.4 Model of bunch occlusion by other bunches..... 37
 - 4.5 Berry and bunch growth factor 38
 - 4.6 Final yield estimation 40

5. CONCLUSIONS..... 45
 Future Perspectives..... 46
REFERENCES..... 47
APPENDIX..... 54

LIST OF TABLES

Table1.Vinbot session during the growing cycle of vines	27
Table2.Average, standard error and yield components at harvest	31
Table3.Number of bunches observed at pea-size and maturation	32
Table4.Relationship between % correlation coefficient and MA%E.....	33
Table5.% of occlusion by bunch and average of occlusion per meter on each phenological stages.....	38
Table6.Average area of berries (cm ²), the average area of bunches (cm ²), the average weight (g) of bunches at maturation, and the growth factors between the phenological stages.....	38
Table7.Values of bunch weight (g) and area (cm ²), at three phenological stages	40
Table8.Average of porosity (%) and average of visible bunches (cm ²), and ± standard error	41
Table9.Formulas used for the yield estimation, for each phenological stages	42
Table10.Relationship between the yield estimated and real yield, for each phenological stages, using the absolute error, percent mean absolute error.....	42

LIST OF FIGURES

Figure1.Spectron (A) and Multiplex (B) hand-device sensors for quality of grape.....	6
Figure2.Representation of yield map	8
Figure3.The RGB model (A), The CIE $L^*a^*b^*$ colour space model (B)	10
Figure4.Workflow of flowers detencion: Data acquisition (A), segmentation of images into 'inflorescence' and 'non-inflorescence' (B), flower extraction(C).....	15
Figure5.Example of the application of the methodology for berry segmentation Original RGB image (A), ROI extracted (B), Berry candidates (C), Final result obtained after filtering false positive (D)	18
Figure6.Example of image processing using the software ImageJ for estimation of projected bunches area (cm ²)	19
Figure7.Map from Google Earth of ISA Vineyard where located the Syrah	21
Figure8.Rainfall and average temperature during growing season 2019	22
Figure9.View of Syrah in ISA Vineyard.....	22
Figure10.Phenological phases of Syrah in season 2019.....	23
Figure11.View VINBOT robot.....	24
Figure12.View of canopy segment on the field.....	25
Figure13.Specific representation of the SPs in the vineyard. The yellow lines were used at pea-size, the green line at veraison, the blues lines at maturation	25
Figure14.Analysis by ImageJ, of bunch on pea-size stage, determining the area of bunch	27
Figure15.Representation of the same vines, at three different level of defoliation on fruit zone (without any defoliation (A), small defoliation (B), full defoliation (C)) at the stage of maturation	28
Figure16.Representation of the same vine, whit (A) and without (B) bunches covered themselves	29

Figure17. Analysis on ImageJ, to estimating the number and the area of berries	30
Figure18. Number of inflorescences and number of bunches at harvest (#/m), and \pm standard error	32
Figure19. Coefficient of correlation and standard error observed between the images and ground truth, \pm standard error	33
Figure20. Relationship between area of bunches (cm ²) (variable independent) and bunches weight (variable dependent), linear regression equations and coefficient R ² , at pea-size stage, n= 60. The * indicates the significant R ² (p<0.000)	34
Figure21. Relationship between area of bunches (cm ²) (variable independent) and bunches weight (variable dependent), linear regression equations and coefficient R ² , at veraison stage, n= 60. The * indicates the significant R ² (p<0.000)	35
Figure22. Relationship between area of bunches (cm ²) (variable independent) and bunches weight (variable dependent), linear regression equations and coefficient R ² , at maturation stage, n= 60. The * indicates the significant R ² (p<0.000)	35
Figure23. Relationship between % of porosity (variable independent) and % of visible bunches (variable dependent), showing the coefficient of determination (R ²) and regression equation, n=20. The * indicates the significant R ² (p<0.000)	36
Figure24. Relationship between % of porosity (variable independent) and % of visible bunches (variable dependent), showing the coefficient of determination (R) and regression equation, n=20. The * indicates the significant R ² (p<0.000)	37
Figure25. Relationship between % of porosity (variable independent) and % of visible bunches (variable dependent), with coefficient of determination (R) and regression equation, n=20. The * indicates the significant R ² (p<0.000)	37
Figure26. Evolution of average area of berries (cm ²) for each phenological stages, \pm standard error	39
Figure27. Evolution average area of bunch (cm ²) for each phenological stages,	

± standard error	39
Figure28.Average of yields (kg/m) using the camera RGB-d Kneticv2 of VINBOT	41
Figure29.Flow chart for yield estimation, for each phenological stages... ..	41
Figure30.Real and estimated values of yield per meter, n= 40	44

LIST OF EQUATIONS

Equation1.NDVI= (NIR-RED)/(NIR+ RED).....	7
Equation2.PCD= NIR/RED	8
Equation3.TGI= $R_{green}-0.39*R_{red}-0.61*R_{blue}$	8
Equation4.VARI= $R_{green}-R_{red}/ R_{green}+R_{red}-R_{blue}$	8
Equation3.Bud fruitfulness index (IF) = inflorescences per burst node.....	11
Equation4.Yield (t/ha) = (IF season/ IF previous seasons) * historical average yield... ..	11
Equation5.Yield (t/ha) = n. of vines * bunches/vine * berries/ bunches *weight/ berry * h. efficiency	12
Equation6.Bunch weight _{harvest} = Bunch weight * berry growth factor	12
Equation7.Berry growth factor= cluster weight at harvest (historical data) /cluster weight (veraison).	12
Equation8.Yield (t/ha)= average yield /vine * number of vines.....	13
Equation9. $Y_{t,c} = (Y_a/T_{t,a}) T_{t,c}$	13
Equation10. $AuB = A+B-AnB \Leftrightarrow AnB = A+B-AuB$	29
Equation11.Occlusion%= $AnB/AuB*100$	29

LIST OF ABBREVIATIONS

ASI= Autonomous solution

CIElab= Color space CIE L*a*b*

GIS= Geographic information system

GNSS= Global navigation satellite system

GPS= Global positioning system

HSB= Hue, saturation, brightness

IF= Fruitfulness index

IPMA= Instituto Portugues do Mar e da Atmosfera

ISA= Instituto Superior de Agronomia

IVV= Instituto da Vinha e do Vinho

LAI= Leaf area index

LIDAR= Light detection and ranging

MA%E= Percent mean absolute error

MAE= Mean absolute error

NDVI= Normalized difference vegetation index

NIR= Near-infrared

NN= Artificial neural networks

PDC= Plant density cell

PQA= Point quadrat analysis

PV= Precision viticulture

RGB= Red, green, blue

ROI= Region of interest

SP= Smart point

TGI= Triangular greenness index

UAV= Unmanned aerial vehicle

VARI= Atmospheric resistant index

VI= Vegetative index

VRC= Vision Robotics Corporation

VSP= Vertical shoot positioning

1. INTRODUCTION

Precision Agriculture is a discipline in agronomy that it was developed on 1980s (Crookston, 2006). This discipline consists of a wide set of techniques and technologies aimed at adjusting crop management and to manage the variability on the field. The characteristics of the crop production, water and nutrients, often vary in space and time within a single agricultural field (Gebbers and Adamchuk, 2010). Therefore, it is important and necessary to take management decisions taking into account these changes. Precision viticulture (PV) is a part of precision agriculture devoted to vineyard management. The use of PV techniques implies the adaptation of fertilizers, phytochemicals and/ or rates of water application to the specific needs of each area in the field (Srinivasan, 2006). The emergence of PV was possible only when significant technological advancements occurred such as, the development of the global navigation satellite system and global positioning system (GNSS and GPS), the development of software designed to manage, analyse and display spatial or geographic data (GIS), the availability of geolocated information remotely acquired (satellite imagery), and the development of variable rate technologies and actuators. The development and use of PV techniques was delayed compared to the other crops, this was due to the intrinsic difficulties of the vineyard characteristics: often there was a heterogeneous canopy from an aerial perspective, which requires higher resolution images, to divide the canopy from the ground, and a greater computing capacity to manage spatial information of the vineyard before being used. PV is mainly concentrated in the delimitation of relatively homogeneous areas. The information about these areas is provided thanks at the use of (a) vegetation indices, that can derived from remotely acquired images, (b) soil characteristics, obtained through non-destructive methods, (c) plant water status, estimated by thermal imaging, (d) previous season geolocated data, (e) RGB (Red, Green and Blue) imaging and other non-destructive sensors, (f) combinations of some of them. These homogeneous areas can be used in order to implement differential management in terms of irrigation, fertilization, cluster thinning and harvest, among other practices (Santesteban, 2019). In the vineyard, vigour, yield and grape quality are variable. This variability can be observed yearly (temporal variability) or in space (local). Knowing this variability can bring advantages to improve the quality of the resulting wine.

Yield estimation in recent years is identified as one of the more important topics in viticulture. A precise yield forecasting could lead to more efficiently managed vineyards producing wines of better quality (Dunn and martin, 2003). A good yield forecast prepares the growers to decide bunch thinning needs, to organize the harvest, to organize the space inside and outside the

cellar, to manage the grape and wine market, to program investment and to develop marketing strategies (Lopes *et al.*, 2016). Yield is determined by yield components such as the number of bunches, the number of berries and the berry weight (Tardáguila *et al.*, 2012). Usually, yield forecasting is conducted using historical yields and weather patterns, along with measurements, monitoring from vines across a given vineyard early in the season (Smart and Robinson, 1991). These methods are usually destructive, labour-demanding and time consuming. Often these measurements do not provide an accurate estimation of the final yield (Diago *et al.*, 2012a). Recently non-invasive imaged-based methods are being investigated to make it possible to efficiently collect detailed information from the vines regarding the yield (Spanling and Miller, 2013). Image analysis can allow the creation of systems capable of estimating the yield without need of contact in a fast and accurate way (Diago *et al.*, 2012a). In recent years, new technologies are being developed for yield forecast using a new ground platform, such as the VINBOT robot, that can provide an accurate yield estimation, using image analysis (Lopes *et al.*, 2016).

Aims of the work

The aims of this work are: to collect data with the VINBOT and analyse the relationship between yield components throughout the season, develop models for estimating the non-visible bunches, estimate yield near harvest and earlier stages of grapevine development, contribute for the development of the ViINBOT platform as a whole by improving its automatic yield estimation algorithms.

2. LITERATURE REVIEW

2.1 Precision viticulture

The concept of precision viticulture (PV) follows the aim to management in different ways the parcels in a vineyard in the real needs of each parcels. A vineyard is characterized by high heterogeneity, causing variability between the vines with consequences on grape quality. Especially in a context of growing competition on international markets, it becomes important to achieve higher quality standard in the vineyard. This heterogeneity involves the use of precision viticulture, maximizing quality and sustainability through the reduction and efficient use of production inputs such as energy, fertilizers and chemicals, ad minimizing input costs while ensuring the preservation of the environment (Matese and Di Gennaro, 2015).

2.2 Monitoring technologies

The aim of the monitoring process is the acquisition of the maximum amount of georeferenced information within the vineyard. Today, a wide range of sensors is available to monitor different parameters that characterize the plant growth environment and are employed in precision viticulture for remote and proximal monitoring of geo-localised data (Matese and Di Gennaro, 2015).

2.2.1 Sensing platforms

The aim of the platforms is to position the detector over the area of interest. The type of the platform is therefore determined by requirements of the measurements to be made. The sensing platforms can be hand-held instruments, or instruments mounted on fixed platforms. Example of platforms are satellites, aircraft, helicopters, drones, robots. Each platforms have own advantages and disadvantages, such as costs, availability, image resolution (Jones and Vaughan, 2010).

The instruments used to acquire all the information of these variabilities (local and temporal) inside the vineyard are cameras, radiometers, line scanner and other sensors. In precision viticulture, the application of these technologies are focused mainly in reflectance spectroscopy. It is an optical technique based on reflectance measurement of the incident electromagnetic radiation at different wavelengths, in particular in visible region (400-700 nm), near infrared (700-1300 nm) and thermal region (7500-15,000 nm). The “spectral signature” is represented on XY graph, where the reflectance value is on the ordinate and the wavelength on the abscissa. Vigour, nutritional status or health of the plants can be detected with multispectral and hyperspectral sensor. Hyperspectral sensing collecting reflectance data over a wide spectral range at high resolution (typically 10 nm), multispectral sensors acquire reflectance data in a reduced spectrum range focused on the red, blue, green, and near-infrared regions with resolution at least 40 nm. The study of the canopy and biomass of the plants can be done by light detection and ranging (LIDAR) system, technology that measures distance by illuminating a target with laser and analysing the reflected light, it can provide a georeferenced 3D reconstruction of each single plant and generate spatial variability maps relate to the size of canopy, directly correlated with the LAI (Leaf Area Index) (Matese and Di Gennaro, 2015).

Monitoring technologies can be separated into two groups: remote sensing and proximal sensing, depending on the distance from which they are being applied. Remote sensing includes aerial imaging while proximal sensing includes sensors deployed from a proximal distance to the analysed object.

2.3 Remote sensing

Remote sensing is defined by the acquisition of data/images from a distance by detecting and recording sunlight reflected from the surface of objects on the ground (Hall *et al.*, 2002). Remote sensing provides information regarding several traits of the grapevine, such as shape, size and vigour and allow assessment of the variability within the vineyard. The data collected at distance allow the description of the plant physiology by calculating the vegetation indices (e.g. NDVI). In remote sensing there are three platforms mainly used, they are satellites, aircrafts and unmanned aerial vehicles (UAVs). The satellite system is capable of providing resolution in visible spectra, in multispectral, in short-wave infrared. Use of satellite in precision viticulture are not sufficient due to the narrow vine spacing, for temporal resolution and cloud cover that can occur at the time the satellite passes. Aircraft is another airborne platform. Use of aircraft bypasses some limitation of the satellite application, such as by programming the

images time acquisition and providing higher resolution, depending of the flying altitude. They can fly under the cloud cover.

The UAVs are called “drones”. They have the capability to fly autonomously means a complex system of flight control sensor (GPS) or controlled by a pilot on the ground. The UAVs give image with high resolution (centimeters), and the possibility of flexible and timely monitoring, due to reduce planning time. The biggest advantage of remote sensing is its capability to collect data very efficiently from a large area, from an aerial perspective (Matese and Di Gennaro, 2015).

2.4 Proximal sensing

Proximal sensing refers to the process of obtaining measurements using monitoring technologies close to the sample. These devices can be used in singular moments or in a continuous manner, when coupled on ground vehicles. There are many tools available for continuous measurements carried by moving vehicles, or instruments for precise ground observations made by operator. Proximal sensing can be used for monitoring the yield, canopy reflectance, berry composition, vigour, temperature of the berry, vegetation appearance, and others.

The growth of technologies has allowed the development of a new kinds of sensors for plant, physiology monitoring, such as dendrometers and sap-flow sensors, sensors for plant water status (Matese and Di Gennaro, 2015). The growers can use these sensors to obtain detailed maps of the spatial variation of the soil properties (McBratney *et al.*, 2001). There are also sensors based on the multispectral like GreenSeeker (NTECH industries, Ukiah, CA, USA) and Cropcircle (Netherlands Scientific Inc, Lincoln, NE, USA). Other sensors can be LIDAR sensors (Matese and Di Gennaro, 2015). Regarding the grape quality there are many tools definite non-destructive based on optical sensors, carried by an operator, using proximal georeferenced measurements. One example of this is the Spectron (Fig.1A) (Pellenc SA, Pertuis Cedex, France), is a portable spectrophotometer with integrated GPS. Used for the monitoring of grape maturation, such as sugar level, acidity, anthocyanin concentration and water content (Matese and Di Gennaro, 2015). Other sensor is the Multiplex (Fig.1B) (Force-A, Orsay Cedex, France), it is an optical sensor that uses fluorescence to determine the concentration of flavonols, anthocyanins, chlorophyll and nitrogen (Cerovic *et al.*, 2008). Comparing to aerial imaging, proximal sensing technologies have the advantage of being able to collect data in a much higher resolution and, in the particularity of row crops such as grapevines, it permits the user to gather data regarding the side of the canopy and not only

its upper part. Proximal sensing includes the cameras, uses for many works in vineyard, such as the yield estimation using image analysis. These cameras can be simple camera as RGB cameras, hyperspectral cameras or multispectral cameras. These cameras can be mounted on a robotic platform (e.g. VINBOT) or used by human operator (Lopes *et al.* 2016).



Figure 1. Spectron (A) and Multiplex (B) hand-device sensors for quality of grape (Source: Matese and Di Gennaro, 2015).

2.5 Robotic platforms

Nowadays, the use of the robots is still at a prototype stage but some robotic platforms have already been in the market. With the innovation and improvement of technology during these years, we will see an increase of use of robots with higher-performance solutions and reduced costs. There are different robots with different purposes that can be used in the viticulture on the future, they are:

- VineRobot project coordinated by Televitis group. This robot is equipped with non-invasive sensing technologies, such as fluorescence sensors, multispectral and RGB imaging for machine vision, thermal infrared and GPS. The system of the robot is designed to perform a proximal monitoring of various parameters such as yield, vigour, water stress, quality of the grapes.
- VINBOT has been proposed by the company Robotnik Automation (Valencia, Spain). The robot has sensors for 3D reconstruction of the canopy and a RGB camera for grape bunch monitoring in order to provide information relevant for yield estimation.
- Wall-Ye has been proposed by Christophe Millot. This robot has a set of optical sensors in order to perform precision pruning.
- VineGuard has been developed by Ben-Gurion University of Negev, Israel. It can navigate throughout the vineyard with a complex set of sensors. The robotic arm designed for grape harvesting uses artificial intelligence to guide the robot in a series of operation like maturation state, localization, selection and detachment of grape from the vine.

- Vitirover is a project developed by Xavier David Beaulieu. This robot is able to cut the grass at the base of the vine. The robot can work independently thanks to a GPS or controlled by computer or smartphone.

There are also prototypes in development proposed by the American company Vision Robotics Corporation (VRC) and by Autonomous Solutions (ASI). These prototypes carry optical sensors that perform a 3D reconstruction of the plants and can carry out very high-detail pruning cuts with two hydraulic shears (Matese and Di Gennaro, 2015).

2.6 Image analysis as a precision viticulture tool

Digital imaging (RGB or otherwise) is a powerful way to collect information and monitor crops with the assistance of automatic systems for their analysis. As mentioned before, these images can derive from satellites, drones, robots or other ground vehicles with optical sensors. Digital images can be used to monitor crops in space and time, with the capability of describing several plants features that can be used to improve vineyard managing by informing the farmer regarding, for example, fruit quality and expected yield (Nuske *et al.*, 2011; Diago *et al.*, 2012a; Nuske *et al.*, 2014; Lopes *et al.*, 2016).

2.6.1 Vegetation indexes

As sensors are used for plant monitoring, digital data is collected in the form of images (RGB or otherwise). This digital image is represented by numerical values that characterize each pixel depending on the energy reflected/emitted by the analysed object. Such values can then be used to compute ratios between them that might give the user information otherwise unknown. These ratios are called vegetation indexes (VI) and can encompass many different wavelengths depending on the sensor used and the type of information aimed by the user.

A commonly used vegetative index is the Normalized Difference Vegetation Index (NDVI). It is calculated in according to the canonical formulation given by Rouse *et al.*, (1974) (Eq.1) and is represented by a value between -1 and +1:

$$NDVI = \frac{(NIR - RED)}{(NIR + RED)} \quad \text{Equation 1}$$

Where NIR (near-infrared) and RED are the spectral reflectance in near infrared and red bands, respectively. In the visible and near-infrared bands, the canopy reflectance, depends on both structural (LAI) and chlorophyll content of the canopy (Zarco-Tejada *et al.*, 2002). The

NDVI can be used as an indicator of plant vigour or relative biomass. For highly vigorous targets, the value of NDVI will be close to unity, and vice-versa (Hall *et al.*, 2002).

Another index is the Plant Density Cell (PDC) (Dobrowky *et al.* 2003), calculated as the ratio of infrared and red wavelengths, it is showed in the Eq. 2:

$$PCD= NIR/RED \quad \text{Equation 2}$$

Indices that represent grapevine’s vegetative development can be used to create vigour or yield maps (Fig. 2) which can be helpful to manage the vineyard based on this spatial differentiated information (Borgogno-Mondino *et al.*, 2018).

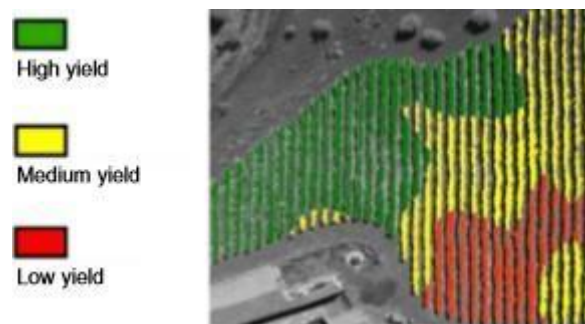


Figure 2. Representation of yield map (Source: Matese and Di Gennaro, 2015).

Previously mentioned vegetation indexes are dependent of multispectral imaging (NIR and IR). Such technology is not always available and can be costly. Several VIs can be computed solely by using visible spectral data (RGB imaging). Some examples of these are the Triangular Greenness Index (TGI) and the Visible Atmospheric Resistant Index (VARI). The TGI (Hunt *et al.*, 2013) (Eq. 3), assesses leaf chlorophyll and plant nitrogen content, while the VARI (Gitelson *et al.*, 2003) (Eq. 4), was designed to work with RGB data rather than near-infrared data. It is a measure of “how green an image is. These indexes are computed as follows:

$$TGI= R_{green}-0.39*R_{red}-0.61*R_{blue} \quad \text{Equation 3}$$

$$VARI= R_{green}-R_{red}/ R_{green}+R_{red}-R_{blue} \quad \text{Equation 4}$$

2.6.2 Colour space

Visible spectral information can be represented in different ways, also known as colour spaces. The most known and commonly used are the RGB (red, green and blue), the HSB (hue, saturation and brightness) and the $L^*a^*b^*$ (also known as CIELAB).

2.6.2.1 RGB (red, green, blue)

Colour can be described in the *RGB* system. RGB is a mixture of the spectra of the three colours red, green and blue. The range of RGB values is from 0 (darkness) to 255 (whiteness). The spectra red, green and blue corresponding at 700, 546 and 436 nm respectively. The system is formed by a cube comprising orthogonal RGB Cartesian coordinates (Fig. 3A). The combination of these three colour can produce all type of colour (Rossel *et al.*, 2006).

2.6.2.2 HSB (hue, saturation, brightness)

The colour is specify in term of three quality, intensity (B) (value or brightness), hue (H) and saturation (S). Hue is the predominant colour, saturation is purity of colour and intensity to its overall lightness or darkness. The HSB can represented around the perimeter of a circle. Around the perimeter are the saturated colour. The central point represents white, formed by admixture of all colours. The intensity can be white ate the centre of the circle and black at the base of the cone. The surface of the cone thus formed represent the saturated colours of different intensities (Jonas and Vaughan, 2010).

2.6.2.3 CIEL a^*b^*

Other method to describe the colour is the *CIELAB* space. This system is obtained after the *xyz* coordinates are transformed to a uniform chromaticity scale. In this system (Fig. 3B) L is the metric lightness function which ranges from 0 (black) to 100 (white), the coordinate a^* is from green to red, respectively $-a^*$ and $+a^*$; the coordinate b^* is from yellow to blue, respectively $+b^*$ ad $-b^*$ (Rossel *et al.*, 2006).

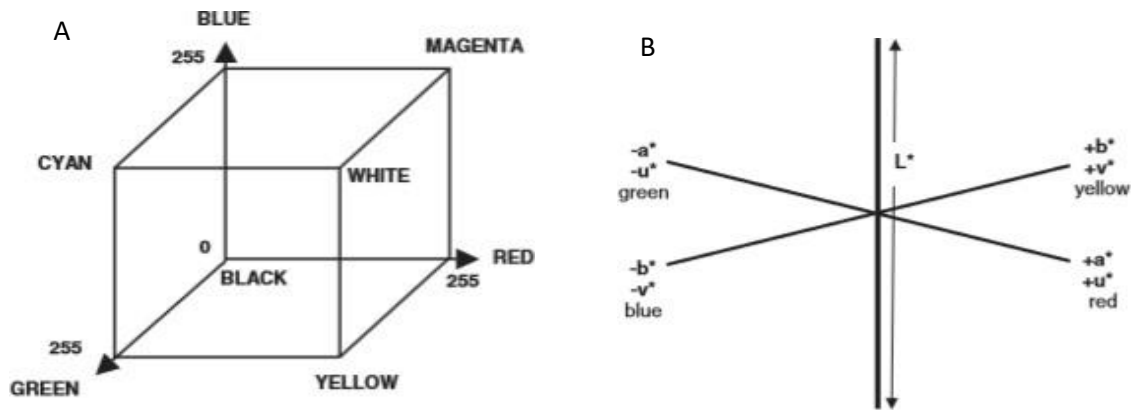


Figure 3. The RGB model (A), the CIE $L^*a^*b^*$ colour space model (B) (Source: Rossel et al., 2006).

2.7 Yield estimation

As previously mentioned, wine/grape production is characterized by a temporal and spatial variability which has consequences for all operations related to the wine business. Consequences as harvest organization, space in the winery, regional pricing negotiation, crusher intake scheduling, investment in new winery capital equipment and the development of marketing strategies for both domestic and export markets. Yield prediction are important to improve the efficiency of vineyard and winery operation (Cunha *et al.*, 2010).

Yield forecasting is still performed using knowledge of historical yields and weather patterns with measurements manually taken in the field. Different studies have established that large spatial variability is present in vineyard, this variability is found between the vines, into a single vine, influencing the vigour and yield forecasting (Taylor *et al.*, 2005). Assuming the spatial variability in a vineyard, often the sample size is too small and inaccurate to estimate the final yield (Nuske *et al.*, 2014).

2.7.1 Estimation method

There are several ways to predict vineyard yield, such as models that forecast yield based on airborne pollen, tension in the trellis system and automatic image analysis. The most common method used in commercial vineyards is the sampling and manual counting of yield components, as number of vines/ha, number of nodes/vine, number of shoot/node, cluster/shoot, flowers/cluster, berries/cluster, berry weight (Martin *et al.*, 2003). This can be

extremely laborious and costly. Forecasts are calculated from data made after budbreak during the season till the harvest.

2.7.1.1 Manual sampling

The manual methods are based on the measurements of all yield components. Using these methods is important to do a well sample in the field. Some of these samples are destructive and time-consuming. The size of sampling first depends on the variability in the field. However, greater the variability, greater is the number of samples required. On the other hand, important is the degree of accuracy required for the samples.

As described above (chapter 2.8.1), forecasting method can be used at a range of times during the season. They are usually applied at particular stages based on yield components, as *early stage*. Early stage can be considered as any stage between budburst and flowering. A very early yield forecast can be made estimating bud fruitfulness before budbreak (Clingeffer *et al.*, 2001). The authors proposed the formulas shown in the equation 5 and 6:

$$\text{Bud fruitfulness index (IF)} = \text{inflorescences per burst node} \quad \text{Equation 5}$$

$$\text{Yield (t/ha)} = (\text{IF season} / \text{IF previous seasons}) * \text{historical average yield} \quad \text{Equation 6}$$

Clingeffer *et al.*, (2001), used the Merbein Bunch Count Method (Antcliff *et al.*, 1972). That method provides an assessment of number of bunches per vine, information on total node number, percentage budbreak, number of shoots, number of fruitful shoots and percentage fruitful nodes.

Yield forecasting can be made estimating the number of flowers (Clingeffer *et al.*, 2001). That method is an indirect method based on allometric relationships between inflorescence length and flower number. That method allows an early forecast of berry number (before bloom) but is very dependent from the fruit set-conditions.

When made at that early time, as flowering, forecast can be inaccurate, the vines will be subject to many factors until harvest including possible environmental hazards, however, if not, such an early forecast can be extremely useful to the farmer. Once inflorescences are fully open other traits can be observed. The number of primary branches is a structural character and it remains more or less constant until flowering. Results from the work of Dunn and Martin (2007) show that the number of primary branches has the potential to detect large seasonal deviation of bunch weight from long term, but with a condition that branch loss do not vary too much season to season. The relationships between the number of primary branches and number of

flowers per bunch remain relatively stable from season to season. An estimate of bunch size based on the number of primary branches can improve yield forecasting made six to eight weeks after budbreak (Dunn and Martin, 2007).

Yield estimation can be made, *after fruit set stage*. One of the main factors affecting the final yield is the number of berries per bunch. This is defined right after flowering, at the fruit set stage. At this stage it is possible to know not only the number of bunches but also the number of berries each bunch has (Clingeffer *et al.*, 2001).

Dunn (2010) proposed a forecast based on berry counts after fruit set. In this case the forecast should be made when the berries are at “pea size stage”. For the Author the formula (Eq. 7) to use is the following:

$$\text{Yield (t/ha)} = n. \text{ of vines} * \text{bunches/vine} * \text{berries/ bunches} * \text{weight/ berry} * h. \text{ efficiency} \text{ Equation 7}$$

The formula means to measure the number of vines, estimate bunches/vine from bunch counts, estimate berries per bunch through sampling bunches, predict average berry weight (at harvest) and lastly harvest efficiency. For the author, forecast based on berry counts after fruit set can expect an error around 10 to 15% (Dunn, 2010). As said above, yield predictions can be attempted at any time during the growing cycle of the vine, but they become more accurate close to the harvest. For that the veraison stage can be a good time to predict the yield. Just like the previous stage forecast models, for estimating the yield, at veraison it is possible to use historical data and berry growth factor. However, at this stage, the bunch is already well developed and close to be harvested.

Using the formulas (Eq. 8 and 9) from Clingeffer *et al.*, 2001, it uses the berry growth factor, through it is possible to predict the final yield.

$$\text{Bunch weight}_{\text{harvest}} = \text{Bunch weight} * \text{berry growth factor} \text{ Equation 8}$$

$$\text{Berry growth factor} = \text{cluster weight at harvest (historical data)} / \text{cluster weight (veraison)} \text{ Equation 9}$$

Harvest samples usually are collected during the week prior to harvest. In proximity at harvest the assessment of yield can be ideal because all the growth stage of crop development have occurred, and in theory, the estimation should provide a good estimate of actual vineyard yield. An accurate yield estimation near the harvest can still be very powerful, as it will help managing the harvest itself and all the logistics related to it. It can also be an effective way to improve wine quality by segmenting the harvest with the resulting prescription maps. Clingeffer *et al.*, (2001), proposed the following formula showed in equation 10:

$Yield (t/ha) = average\ yield /vine * number\ of\ vine$

Equation 10

2.7.1.2 Airborn pollen method

At flowering stage, yield forecasting can be made using airborne forecast models. That model is valuable tools for the yield estimation, because it put simultaneously several factors that influence the crop production: preflowering conditions, plant vigour and health. (Besselat and Cour, 1996). There are the possibility of create forecast model for grape production based on concentration of the pollen in air. It is explained in several studies. One of this was conducted in S. Michele all'Adige (Italy). In this research the authors used, instead of a Cour trap usually adopted in this type of research (Cunha *et al.*, 2003), the Hirst-type sampler, which permits the determination of daily airborne pollen concentrations ($P/m^3/day$). For a better result, the concentration of pollen was collected for a five year. To improve the model was important to recorder meteorological parameters, in particular rainfall during the main pollen season, the temperature immediately preceding pollination, because rainfall can influence negatively the beginning of the pollen season (Cristofolini and Gottardini, 2000).

In another study, Cunha *et al.*, (2003) for the concentration of airborne pollen used the Cour trap. In the Cour method, pollen grains are trapped on vertical gauze filters with an area of $400\ cm^3$ fixed vertically on a wind-vane, which continually orientates the filters according to the wind (Cour 1974). In this case during the flowering the filters are exposed for 3 or 4 days in the air. Airborne pollen is express in number of pollen grains transported per m^3 of air. The model show a good results in crop prediction, but the main disadvantages of this forecast are the placement representative of the airborn pollen sampling device at regional level and complex laboratory process involved (Cunha *et al.*, 2003).

2.7.1.3 Trellis tension method

In a work from Blom and Tarara, (2009), it has been seen that can be used the trellis tension for the monitoring of the yield. The trellis tension monitor was developed using the tension of the horizontal support wire of trellis. The authors used the formula (Eq.11) to predict the final yield using the known yield and trellis wire tension value from antecedent years:

$$Y_{t,c} = (Y_a / T_{t,a}) T_{t,c}$$

Equation 11

Where $Y_{t,c}$ is the predicted at any time (t) of the current year, Y_a is the yield from an antecedent year, $T_{t,a}$ is the trellis wire tension at the time t from the antecedent year, $T_{t,c}$ is the wire tension at time t of the current year. The authors say that for apply is necessary to have several

historical data and over time the accuracy of the yield estimation from trellis tension system will be improved. The results show that it can be used to supplant the traditional, labor-intensive, yield estimation practices or to supplement longstanding practices with real-time information that can be applied to dynamic revision of static yield estimation.

2.7.1.4 Agrometeorological models

Agrometeorological models are obtained from the regression between climatic variables measured in a determinate phenological phase. These models assume that the climatic conditions are the main factor of the variations of the yield. According to Gommers, (1998), these models can be obtained through descriptive methods, regressions or yield simulations. The regression models use the main important climatic variables, such as air temperature and precipitation. Using the harvest simulation, describes the behaviour of the crop based on the meteorological conditions which it is subjected. These models are very variable and difficult to extrapolate, for that they are less used in yield forecasting.

2.7.2 Image analysis

As mentioned previously, the most commonly used yield forecasting methods described above are destructive, laborious, time demanding and expensive. In recent years several studies are based on image processing in order to assess the yield estimation or other features of the vineyard canopy. The technology of image analysis allows the creation of systems capable of estimating yield without the need of contact in a fast, repeatable and accurate way (Diago *et al.*, 2015). Image analysis means to analyse what is in one image. The acquisition of the image on the field can be done manually (Diago *et al.*, 2012a), or with modified agricultural vehicles such as robotic platforms or other ground vehicles as mentioned before (Lopes *et al.*, 2016). One of the first works about image analysis, from Dunn and Martin (2004), had the objective to detect differences in visible characteristics between fruit and other elements of grapevine canopies. This work showed that fruit can be distinguished from other part of the canopy by image analysis and the fruit pixels could be counted to provide a quantitative measure of the amount of visible fruit in each image (Dunn and Martin, 2004). More works are made during the season taking as yield components flowers (Diago *et al.*, 2015; Rudolf *et al.*, 2018), berries or bunches (Tardáguila *et al.*, 2012; Nuske *et al.*, 2014; Herrero-Huerta *et al.*, 2015; Aquino *et al.*, 2017). Other authors conducted works to estimate the yield based on shoot detection using videos acquired by cameras moved along the row (Liu *et al.*, 2017).

2.7.6.1 Image analysis to detect the flowers

As said previously, the number the inflorescence and the number of flowers are important parameters to estimate the yield, because the flower become berries. Counting the flower number per inflorescence is essential for accurate assessment of fruit set. To improve the quality of the forecasting, in recent years, several studies were based on the use of image analysis using inflorescence in order to predict the yield in early stage (Diago *et al.*, 2014, Aquino *et al.*, 2015; Millan *et al.*, 2017). Diago *et al.*, (2014) used RGB images taken under field conditions to estimate the number of flowers per inflorescence. The authors of this work processed the images using Matlab (MatlabR2010b, MathWorks, Natick, MA, Usa). The method developed for flower counting was fully automatic and involved three stages, for first the images were pre-processing involving conversion of the image from RGB to CIELAB colour space, and an initial segmentation by means of threshold, separating by background from the flowers. Second step was the flower counting, and as the flowers present a higher degree of light reflection, the flowers corresponded to brighter areas. The last step was to remove material other than flowers from the brighter area selected. The authors validated the results from the software, counting manually the flowers number and compared that data by software. Others authors, such as Rudolph *et al.*, (2018), had a different approach to estimate the number of the flowers. They estimate the flowers number taken the images in field conditions without background. The work was divided into four steps, the first simple-to-handle image taking with camera, the second was identification and localization of the inflorescences with segmentation of the images, after extraction of the flower and finally the evaluation of resulting phenotyping data. The figure 4 show the workflow for flower detection:

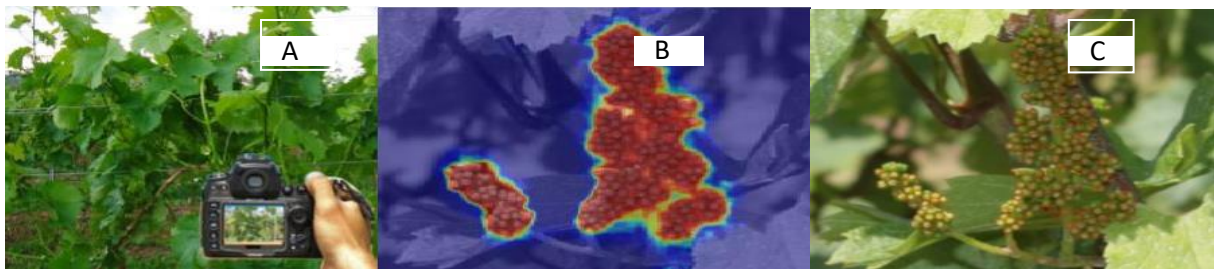


Figure 4. Workflow of flowers detection: Data acquisition (A), segmentation of images into 'inflorescence' and 'non-inflorescence' (B), flower extraction (C). (Source: Rudolph *et al.*, 2018).

2.7.6.2 Image analysis to detect the bunches and berries

As described above, the number of berries is one component involved in the final yield determining also the cluster compactness, cluster architecture and degree of berry aggregation (Cubero *et al.*, 2015). Many works explained how to count the berries by image analysis. Grossetete *et al.*, (2012) used a digital camera and a simple Smartphone, from flowering to veraison, to do the photos and analyse these to counting the berries. The photos were made using camera with integrated flash, because the berry surface reflect the light and the maximum point of reflection was on the centre of the berries. The images were processed as following: the correlation between the Gaussian profile and the neighbourhood of each pixel was computed, the result is called correlation maps; that was thresholded; the last step consisted in a morphological dilation in order to solve the situation where specular areas could occur on a single berry. At the end of the process, the authors obtained the number of visible berries.

Diago *et al.*, (2012a), used RGB images taken in the field to assess leaf area and yield estimation. For the development of their Algorithm was used the Mahalanobis distance. The Mahalanobis distance has been found to be the most suitable and widely used for pattern recognition and data analysis (Son *et al.*, 2010). The Mahalanobis colour distance standardizes the influence of the distribution of each feature considering the correlation between each pair of terms (Al-Otum, 2003). In the experiment of Diago *et al.*, (2012a) the vines were randomly chosen and defoliated and cluster thinned in several steps. The pictures were made before and after any defoliation and cluster thinning. To avoid confounding effects from background and no artificial illumination, it was placed behind the canopy a white background. The method processed sets of images, and calculated the areas (number of pixels) corresponding to different classes like grapes, wood, background and leaf. Each one was initialized by the user, who selected a set of representative pixels for every class in order to induce the clustering round them. For the Algorithm validation, it was manually performed, selecting ROI (region of interest) on images that showed representative conditions of illumination and colours. The ROI selected, the number of pixels for each class was manually counted. The segmentation results showed a performance of 92% for leaves and 98% for clusters, allowed to assess the leaf area and yield with R^2 values of 0.81 and 0.73, respectively.

The work of Nuske *et al.*, (2014) was used a RGB camera, artificial illumination mounted on a tractor. The yield estimation was made before veraison. The aims of that work was to develop an algorithm to detect the berries to known the final yield. Their approach was to detect candidate hypotheses of where grape may be located in the images. To detect the potential berry location they used two ways, the first was radial symmetry (Loy and Zelinsky, 2003) that

uses the circular shape of berry as a cue for detection. The second was the search of the maximal point of shading in the centre of grapes, it was illuminated by flash. The next step of their algorithm was to classify the detected key points into grapes or not-grapes. The authors manually defined the berries centres that corresponded to positive examples of the appearance of berries and they removed bunches of detections that were smaller than an area threshold. The next step of this work was to take the measurements of the berries and make an estimating of fruit yield, evaluating the visible berries and berries self-occluded. They did it in two ways, the first, they took convex hull formed by all the visible berries in the bunches. The second way was to predict the size of a bunch using a 3D ellipsoid model. The authors, in the laboratory environment, collected image from ripe clusters, weighed and counted berries number. Initially they compared the total berry count (manually) of each cluster against its weight. After, it was started with the visible berry count, and by ellipsoidal model the authors said that was a lower correlation than the visible cluster. Ellipsoidal model does not assume that the clusters do not have uniform density or the clusters are not ellipsoidal. Subsequently, the authors compared their automated berry counts with the harvest crop weights (Nuske *et al.*, 2014).

Others works, for estimate the yield, use images in 3D. From an image 2D from the field of bunches, it is possible to produce an image 3D, to know the bunch weight and number of berries. That work is explained by Herrero-Huerta *et al.*, 2015, with the aim to remove the subjectivity deriving from the spatial and temporal variability of the grape production. For this type of work, they were difficulties, such as having only the visible side of the bunch, or having deal with the occlusion and geometrical complexities of the bunches themselves. In that case it was important the acquisition of the image such as their position (spatial and attitude), because will affect the final accuracy (in term of prospective ray intersection) and completeness in terms of overlap between image) of the 3D. To reconstruct the bunches in 3D model, the images was processed with Photogrammetry Workbench software developed by the authors (Herrero-Huerta *et al.*, 2015).

Aquino *et al.*, (2017), used the 2D image analysis to estimate the number of berries per bunches. The authors divided the work on two step, for first they extracted a set of berry candidates from the image by means of a morphological filtering, the bright spots produced by the light reflection on the berries surface were detected by finding regional maxima illumination. Second step was that the candidates not corresponding to berries, false positive, were discard. The images were converted into CIELAB colour space (CIE 1976 L*a*b*) (Connolly and Fleiss. 1997). To obtain the berry candidates, the authors used a dark background, it enables easier extraction of a region of interest (ROI) by means of colour discrimination, and the ROI was extracted from the image by thresholding of the channel b* using the Otsu's thresholding

method (Nobuyuki, 1979). The ROI included also errors, other components, such as rachis, to discard these errors was used a filtering. The filtering process was carried out by means of pixel classification. In the second step of this work, it was remove the false positive. The components that corresponded to false positive were manually labelled in red colour. After, was used the Neural Networks (NN) approach, created by assigning the 0 and 1 value to the red and blue components, respectively. NN produces real values, is needed to obtain a classification result by assigning the values 0 and 1 to false and true positive. The authors, considered that the values produced by the NN for each connected component were as probabilities and used to create a probability map in form of an image. After, this new image was binarized using the threshold automatically provided by Otsu's method (Aquino *et al.*, 2017). The Figure 5 shows an examples of these application of the whole described methodology step by step.

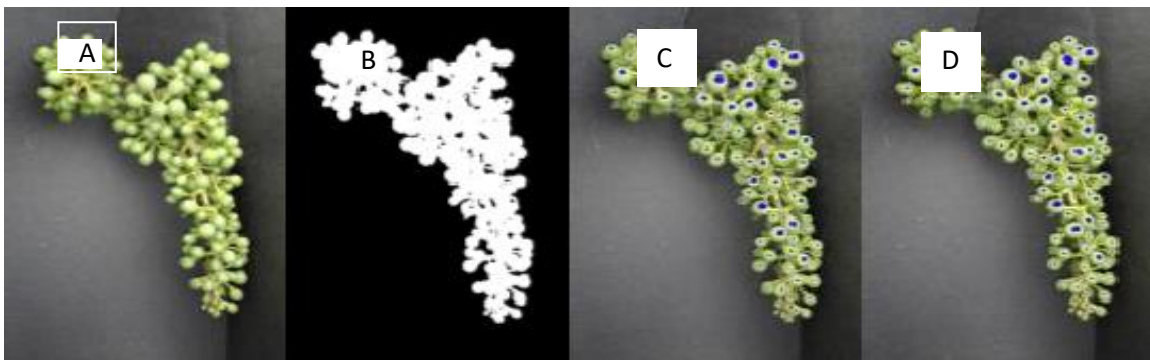


Figure 5. Example of the application of the methodology for berry segmentation. Original RGB image (A), ROI extracted (B), Berry candidates (C), Final result obtained after filtering false positive (D) (Source: Aquino et al., 2017).

Artificial neural networks (NN) was used also in a work of Behroozi-Khazaei and Maleki (2017) to develop an algorithm to segment bunches. The photos were made in a plant cover by leaves and near harvest. The authors obtained the 99.4% accuracy for their algorithm.

Lopes *et al.*, (2016), used a new robotic platform, called VINBOT, focused on yield estimation. The authors manually assessed canopy dimensions and yield (bunch number and weight) and then scanned by the VINBOT. They analysed the images using an image analysis algorithm (ImageJ 1.48V). The total area occupied by bunches in the image was computed in pixel and then converted into actual cm^2 (Fig.6). The last steps of that work was to convert this area into kilograms.



Figure 6. Example of image processing using the software ImageJ for estimation of projected bunches area (cm^2) (Source: Lopes et al., 2016).

2.7.6.3 Image analysis to detect the canopy features and porosity

Canopy porosity, also known as the percentage of gaps in the canopy, is an important vegetative trait. It affects grape bunches regarding sunlight capture, shading, airflow (which reduces the chance of fungal diseases, Austin *et al.*, 2011), synthesis of aroma/flavour compound (Reynolds and Wardle 1989; Diago *et al.*, 2010), synthesis of phenols compound, as anthocyanin (Bubola *et al.*, 2012, Diago *et al.*, 2012b, Tardáguila *et al.*, 2012). Ideal grapevine porosity was defined to have 10 or 20 % (Palliotti and Silvestroni 2004) or 20 to 40% gaps (Smart 1987). The traditional way to evaluate canopy porosity is the Point Quadrat Analysis (PQA, Smart 1987), which consists in the insertion of a probe through the canopy (perpendicularly) and counting the number and parts of the vine the probe comes into contact with (leaves, bunches, canes or gaps). This assessment of canopy porosity is laborious and time consuming and can potentially damage the fruits. Images analysis was used by Tardáguila *et al.*, (2012), in a work to assess the canopy features of vineyard. The authors, to evaluate the canopy features, at harvest, after image acquisition, assessed the leaf area using a leaf area meter in the laboratory. The photos were made using a digital camera and a white background to avoid noise from the grapevines of the next row. First the digital images were cut out to include only the portion of canopy corresponding to the vine. These images were analysed with the program Matlab (Mathworks, USA). The program works with a selection of user defined pixels on the images as a starting point for a classification algorithm based on Mahalanobis distance (Tardáguila *et al.*, 2011); it establishes classes like bunches, green leaves, yellow-wilted leaves and canopy porosity. This program count automatically the total number of pixel in each class. The authors of this work confirm the strong relationships between the yield and total leaf area using computer vision (Tardáguila *et al.*, 2012). In a recent work from Diago *et al.*, (2016) a new methodology to assess the canopy porosity, using the help of image analysis, is explored. Images were collected with a commercial digital

camera and a white background and image analysis was conducted in order to estimate canopy porosity digitally using the Mahalanobis distance to classify gap pixels. A linear regression was then used between PQA values and porosity calculated through image analysis, showing very good results ($R^2=0.93$).

2.7.6.4 Challenges to overcome

The image analysis from the images acquired in the field have to be a challenging, this because in the field the scenario is uncontrolled. One of this challenging is to improve the segmentation process of image for the unevenness in the berry (Nuske *et al.*, 2011), another important challenging to improve is that not all the berries in a cluster are visible, this due to the occlusion from other berries, leaf or other material from the vine, for this many works are destructive (removing the leaves, cluster thinning). To overcome these problem, Millan *et al.*, (2018), used a Boolean model. The advantage of that model is the capability to estimate the number of particles present in an image, even when errors in the segmentation or occlusion are present. The Boolean model was developed by Matheron (1975) and Serra (1980).

2.8 Vinbot

The VINBOT is a new robot developed according to the EU Strategic Research Agenda For Robotics in Europe 2014-2020. VINBOT (Autonomous cloud-computing vineyard robot to optimise yield management and wine quality) has the ability to capture and analyse images and 3D data, thanks to set of sensors, by means of cloud computing application, in order to obtain the variability in vineyard in term of yield. The first experiments with the VINBOT were set up in an experimental vineyard in Lisbon. Results were very positive regarding vegetative traits, such as exposed leaf area and leaf area index, however an underestimation was observed when attempting to estimate the yield (error of 15.2%) and the relationship between ground truth and estimated yield was average ($R^2=0.31$) mainly due to the effect of bunch occlusion. Further research is required in order to improve the results of this platform. As shown earlier, algorithms to detect yield components in digital images taken from real conditions are already very advanced and with low errors, nevertheless, in order to perform a full yield forecasting, the research must address the problem of bunch occlusion (Lopes *et al.*, 2016).

3. MATERIALS AND METHODS

3.1 Localization experiment

The vineyard is located at “*Instituto Superior de Agronomia*” (ISA), in Lisbon, with the coordinates 38°70'92.86"N, 9°18'72.42"W and 62 m above sea level (Fig. 7).



Figure 7. Map from Google Earth of ISA Vineyard where located the Syrah.

In ISA there are two vineyards located on two different plots, one for white varieties, such as Macabeo, Moscatel Galego, Moscatel de Setubal, Alvarino, Viosinho, Encruzado and Arinto, and another one with red varieties. Regarding the plot with red varieties, they are different geographical origins, from Portugal such as “Touriga Nacional” and “Trincadeira” and French cultivars “Cabernet Sauvignon” and “Syrah”. The plot have a slope of 11%.The soil is a clay loam with 1.6% organic matter and a pH of 7.6 (Monteiro *et al.*, 2018).The vines are spaced 1.2 m within and 2.5 m between north-south oriented rows and trained to a vertical shoot positioning trellis with two pairs of movable wires, and spur-pruned on a bilateral Royal Cordon system. The climate of Tapada da Ajuda is, according to the characterization of Thornwaite, mesothermal, with moderate rainfall in winter and deficit in summer. In 1971/2000, the average of annual temperature values were 16.4 °C, with an average minimum value of 11.8 °C, recorded in winter and an average maximum of 21 °C obtained in the summer. Average annual of rainfall was 725.8 mm, with maximum values recorded during the winter months and minimum values during the summer months (IPMA 2019). The figure 8 shows the evolution of precipitation and average monthly temperature at Tapada da Ajuda during the season 2019,

which the wettest month was April. Rainfall were below the average for the last 30 years. The high temperatures occurred during the cell growing phases, they determined that some bunches were loses (IPMA 2019).

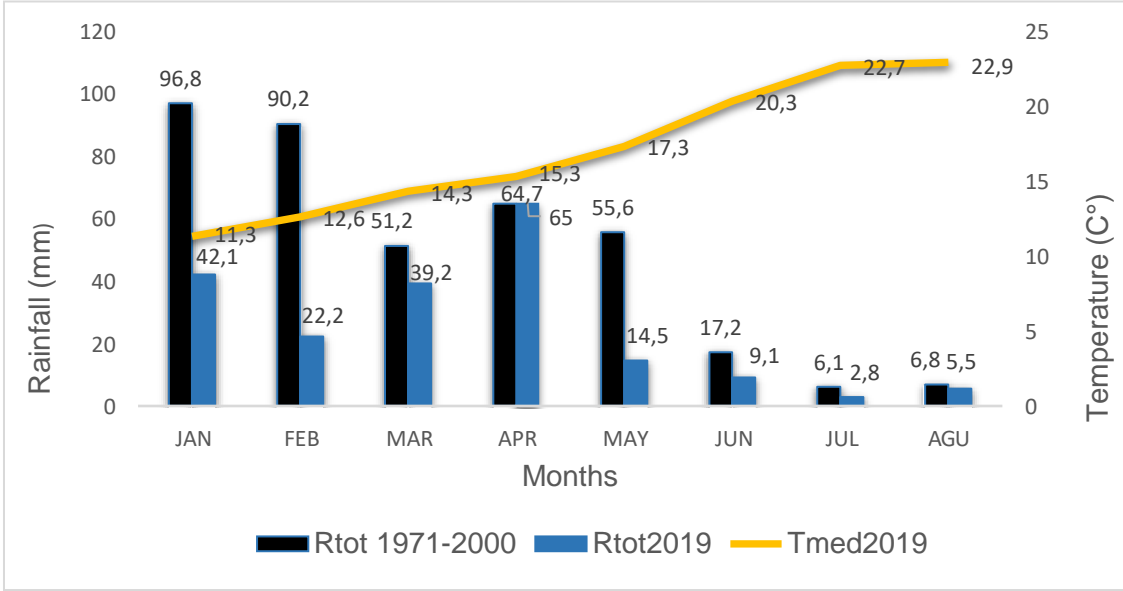


Figure 8. Rainfall and average temperature during growing season 2019. (Source: IPMA 2019).

The trial of this study was carried out whit the variety Syrah (Fig. 9). In ISA vineyard Syrah was planted on 1998 and grafted onto the 140 Ru rootstock. For the validation purpose it was used only the vertical shoot positioning (VSP) system, commonly used in most part of the world winegrowing. The variety has high vigour, high fertility of basal buds and low or very low intensity of anthocyanin pigmentation. The Syrah shows an average length, weight and compactness with a conical shape with numbers of wings ranging from one to two. In terms of berries, it has a medium size with a short elliptical shape, with an unpolished pulp and a soft consistency. In terms of yield, it shows a medium productivity, it can be high in some clones (cl.99 Fr; cl.100 Fr). Regarding the diseases, that variety is medium sensible at *botrytis*, *oidium*. It is sensitive at chlorosis (IVV, 2011).



Figure 9 View of Syrah in ISA vineyard.

The 140 RU (Berlandieri x Rupestris) is a rootstock with high vigour. It is more resistant to dryness and at the presence of limestone (Fregoni, 1999).

Figure 10 show the phenological phases of Syrah during growing season 2019 in the ISA vineyard.

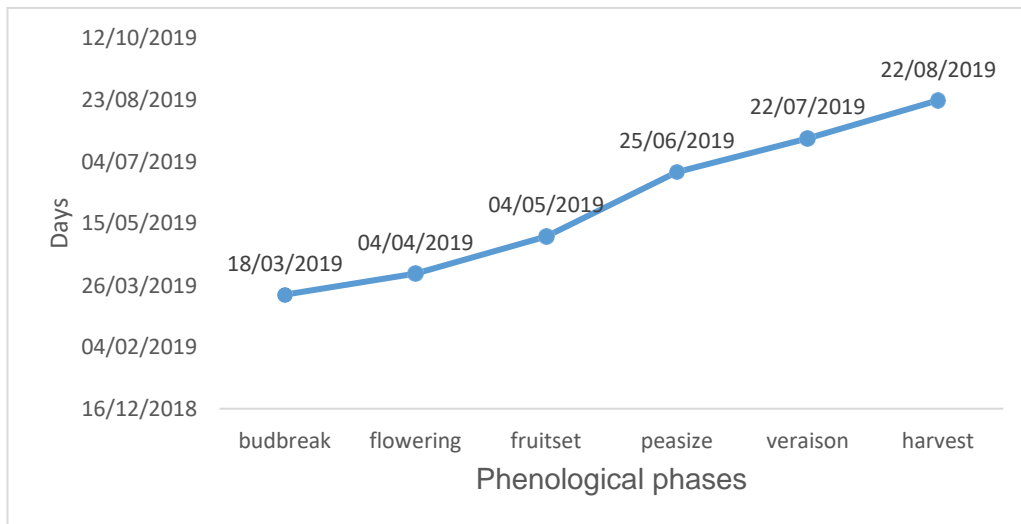


Figure 10. Phenological phases of Syrah in season 2019.

3.2 Vinbot

The VINBOT robot (Fig. 11) was projected with the purpose of collecting real field data, as yield components, leaf area, and comparing them with the estimates provided by the autonomous VINBOT system. Robot's platform is based on a commercial robot Summit XL HL, it can carry up to 65 kg. Platform is durable, mobile, at beginning was developed on ROS Indigo Igloo, actually in ROS Kinetic Kame, developed for the robotic. VINBOT have an RGB-D Kinect v2 camera to take images, have a Laser rangefinders (LiDAR) Hokuyo UTM-30LX Scanning, used for the navigation and to obtain 3D reconstruction of canopy. It have a computer for basic computation functions, connected to a communication module. The robot is capable to navigate autonomously in the fields, it can climb up on 45°. It have a battery capacity of up to 8 hours. About the navigation, can be used a laser range finder and RGB-D device to perform reactive row following and obstacle, and traditional RTK-DGPS where the robot follows a set of pre-programmed waypoints (<http://www.vinbot.eu>).

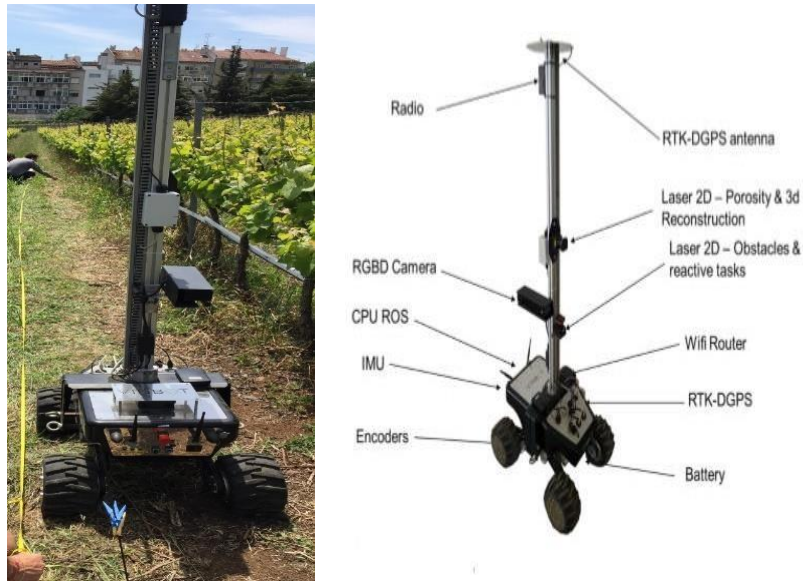


Figure 11. View VINBOT robot.

3.3 Cultural Practices

As cultural operations were practiced during the biological cycle, they were followed by a team of technicians from the “*Instituto Superior de Agronomia*”, these practices were the same for all plots and do not interfere with the results of this study.

3.4 Experiment design

In ISA vineyard’s, randomly was chosen the rows and the vines, taking into account the spatial variability along the vineyard and along the rows. The rows chosed were the numbers 14-15-16-18. For each rows were considered 10 linear meters, these weren’t subject at cultural practices as defoliation or bunches thinning. These canopy segments were called smartpoint (SP), they were labelled by a measuring tape (10 meters) attached to the base of each vine, to allow a better identification of images and provide a known scale per each photo (Fig. 12). SP1 and SP3 was at beginning of the respective rows (numbers 14-16), the SP3 and SP4 was at the end of the rows number 15 and number 18 (Fig.13). These SPs were used to be photographed by VINBOT at predefined phenological stages as budbreak, visible inflorescences, pre-bloom, pea size, veraison and maturation.



Figure 12. View of canopy segment on the field.

Others segments were chosen for each rows (numbers 14-15-16-18), 5 meters on each phenological stage, in totals 15 meters (5+5+5), to evaluate the detailed measurement and analyses destructives for three predefined phenological stages, pea size, veraison and maturation. For this purpose, each steps were performed by the Nikon D5200 camera, at different level of defoliation (low, medium and full defoliation). On these segments it was chosen one meter to harvest the bunches, these were weighted and analysed in the laboratory. Each bunch was identified with the label. The bunches in laboratory of ISA were photographed, manually were calculated the volume. Each bunch was destemmed and photographed by a normal compact camera.



Figure 13. Specific representation of the SPs in the vineyard. The yellow lines were used at pea-size, the green line at veraison, the blues lines at maturation.

3.5 Methodologies

During the vegetative season, VINBOT sessions were made for each SP's previously chosen, in the data of all phenological stages predefined (Tab.1) and the RGB images were captured only in a sides of the lines, with a distance between the VINBOT and vines at 70-80 cm. The trials were carried out from early stages, the first trial was at stage of 4 leaves, until the maturation. The aim was to compare the yield components presents between the ground truth and the images from the VINBOT, both with blue background and without background. These trials were carried out from early stages of development in order to find possible correlations that would allow as to reach the goal of estimation yield as soon as possible in relation whit the harvest. On each SP's, from pre-bloom until maturation was assess the porosity. The porosity was estimate, using the blue background, and analysed it by the software "ImageJ", as explained in the appendices A. From pea-size stage until full maturation it was estimate the area of visible bunches.

At the stages of pea-size, veraison and full maturation were made the detailed measurements. The images RGB were taken out by camera Nikon D5200. For first step the photos were made without any defoliation. For each smart point was choose the level of defoliation, that was small defoliation, medium, hard and randomly, respectively SP1 small, SP2 medium, SP3 hard and SP4 random.

The bunches were harvested and weighted. Bunches were taken out in bases on the occlusion of each bunch, in that case was divided in layers. For each 5 meter, only in one meter representative, was harvested, labelled to be analyse in the laboratory. That bunches in the laboratory were photographed in two prospective using the blue background, weighted (bunches and berries) using a KERN scale (KERN FCB Version 1.4), calculated the volume.

The images RGB both captured by VINBOT and Nikon D5200 were analysed with software "imageJ". In this software, which is a freeware software, developed by the National Institute of Health of the United States of America, the image can be analyse, modify, process, record and print 8-bit, 16-bit and 32-bit image. It performs standard image processing, including contrast manipulation, sharpening and contour detection. It calculates areas, porosity, measure distance and angle, as well it produces density histograms and linear graphs.

3.5.1 Analysis of yield components

In order to collecting the images of vines, that better predict the yield, it was performed by the VINBOT robot and NikonD5200 in the phenological stages shown in Table 1. The sessions

were performed controlling the robot position at a distance more or less of 70 cm from the row, selecting speed on the controller (the speeds were three) and maintaining the measuring tape in front of the camera. On each images captured, it was performed the actual verification on the field of the number of shoots, number of inflorescence, number of bunches, taking into account the respective phenological stage. In each images it was performed the number of yield components, porosity and area of visible bunches. For each phenological stage analysed, the coefficients of correlation between the ground truth data and data from images were found. All the images captured were analysed manually using the software “ImageJ”, as indicated in A.1.

Table1. VINBOT session during the growing cycle of vines.

VINBOT session	4 leaves	Inf.	Pre-bloom	Pea-size	Veraison	Maturation
Data	28- 29/03/2019	04/04/2019	29/04/2019	25/06/2019	22/07/2019	23/08/2019
Yield component	N.of shoots	N. of inf.	N.of inf.	N.of bunches	N.of bunches	N.of Bunches

3.5.2 Projected area of bunch and bunch weight

In order to estimate the weight of bunches from the projected area (cm²), in the laboratory images were captured from two different sides. The analysis was made at pea size stage, veraison and full maturation. The photos were captured by Nikon D5200 in laboratory from two background, perpendicular to each other. For each stages, for each SP on 5 meter was chosen one meter representative and was captured 60 images. These images were analysed manually by ImageJ (Fig. 14), as showed in A.2. The area of each bunch (cm²) was transformed into kg. All the bunches were weighed in the laboratory, by a scale of precision KERN FCB 3K0,1, and data were registered in EXCEL software.

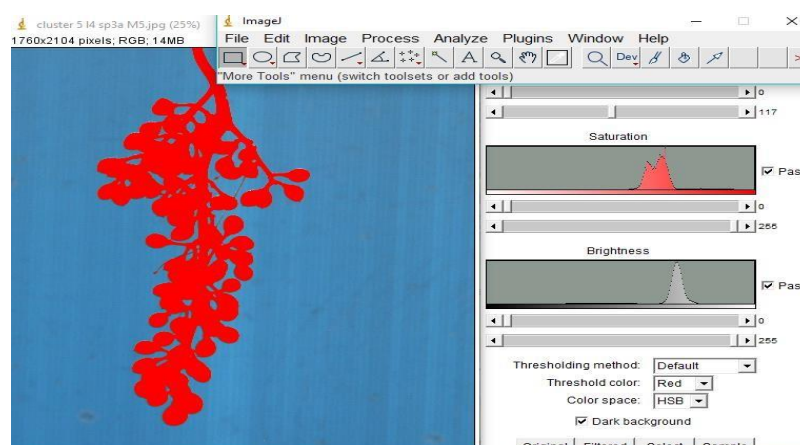


Figure 14. Analysis by ImageJ, of bunch on pea-size stage, determining the area of bunch.

3.5.3 Model for bunch estimation covered by leaves

The numbers of visible bunches depends on the porosity of the canopy, which influences the accuracy of yield. The porosity was calculate in %, higher % of porosity higher is the % area of visible bunch. The porosity was assess using images by Nikon D5200. The RGB images were captured in different levels of defoliation on fruit zone, that was small defoliation, medium, hard and randomly, respectively SP1 small, SP2 medium, SP3 hard and SP4 random. The photos were made before and after any defoliation and using a blue background (Fig. 15). All the images were analysed with the software ImageJ, as indicates in A.3. On each images it was evaluated the porosity and the percentage of visible bunches. The estimation of bunch covered by leaves was calculated as area of bunches on the images (cm²) divided by the area of the same images without leaf (cm²).



Figure15. Representation of the same vines, at three different level of defoliation on fruit zone (without any defoliation (A), small defoliation (B), full defoliation (C)) at the stage of maturation.

3.5.4 Model of bunch occlusion by bunch

Bunches can occlude other bunches; for a better yield estimation it was estimated the area of bunches occluded by other bunches. The images RGB was captured by Nikon D5200 camera, on 5 meter of each SP, after total defoliation in the fruit zone, at pea size stage, veraison and

full maturation. The camera for each meter was kept in the same position in front of the meter where the images were captured, initially with all the layers of bunches, after the removal of layers of bunches that covered other bunches. The photos were made using a blue background and a meter was positioned to precisely identify the length of the meter to be photographed. All the images captured were analysed manually by software ImageJ (Fig. 16), estimating for each images the total area of bunches in the images, the area of bunches removed in each level and the percentage of porosity. To assess the occlusion % was used equations 12 and 13:

$$A \cup B = A + B - A \cap B \Leftrightarrow A \cap B = A + B - A \cup B \quad \text{Equation 12}$$

$$\text{Occlusion \%} = \frac{A \cap B}{A \cup B} * 100 \quad \text{Equation 13}$$

Where **AUB** is the image with all the layers, **B** is the image without a layer, **A** is what we took away.

The images were analysed as indicate in A.3.

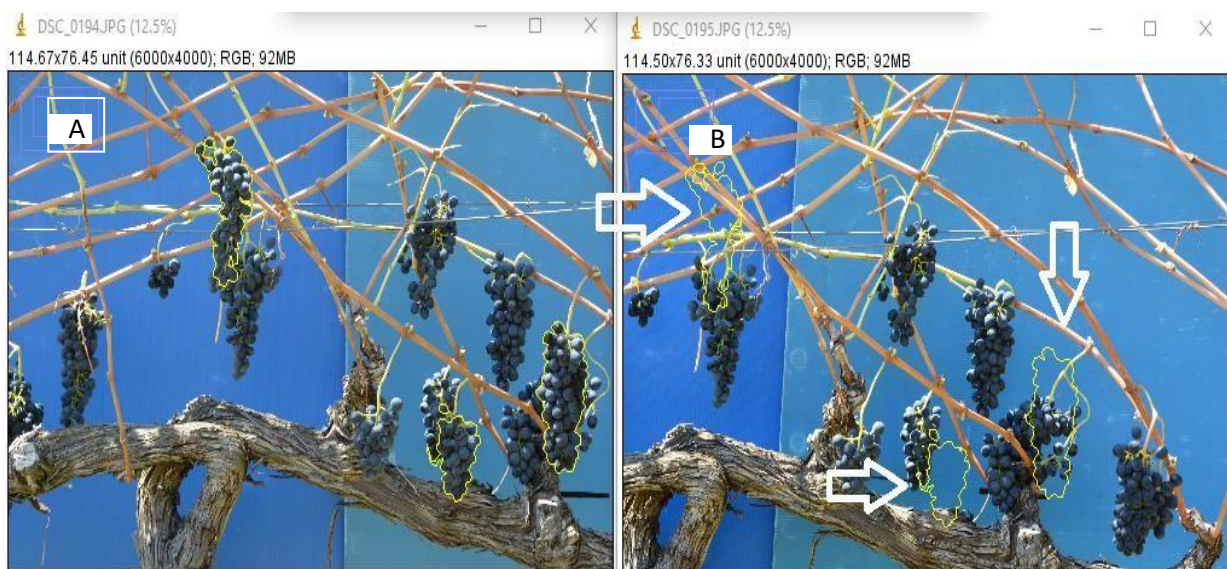


Figure 16. Representation of the same vine, whit (A) and without (B) bunches covered themselves.

3.5.5 Berry and bunch growth factor

In order to estimate the berry growth factor during the cycle of vines, bunches were destemmed, the berries of each clusters were kept on a table background to be photographed by compact camera in the laboratory. The photos were made from bunches harvested on the meter chosen of 5 meter for the detailed measurement at the stage of pea size, veraison and maturation. The images were analysed by the software Image J (Fig.17), as indicates in A.4. At each stages it was assess the area (cm^2) of the berry and calculated the berry growth factor.

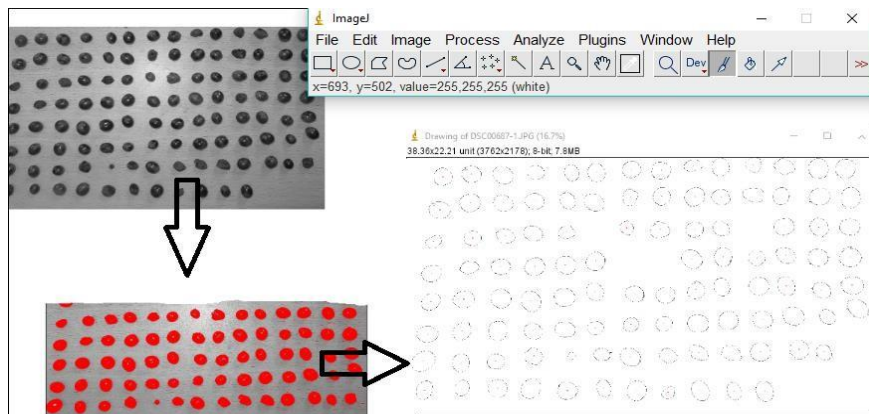


Figure 17. Analysis on ImageJ, to estimating the number and the area of berries.

4. RESULTS AND DISCUSSIONS

4.1 Analysis of yield components

At harvest, the yield per meter and the numbers of yield components observed are show in the table 2. The yield was 0.81 kg/m, the highest yield was found in SP4 with average of 1.11 kg/m, the lowest value was found in SP2, it showed an average of yield of 0.61 kg/m. These differences explain the high spatial variability inside the vineyard, the vines on SP4 had high vigour than other rows. Regarding the number of bunches per meter, in SP4 showed the highest number with a mean of 18.5 bunches per m, the lowest number was in SP2 with a mean of 12 bunches per meter.

Table 2. Average, \pm standard error and yield components at harvest.

Bunches (#/m)	Yield (kg/m)	Bunches weight (g)
15.28 \pm 0.24	0.81 \pm 0.38	42.38 \pm 0.30

During the growing cycle of vines, other observations in the field were performed at predefined stage as number of shoots per meter, number of inflorescence per meter and number of bunches per meter. The number of shoots observed were 12 shoot/m.

The number of inflorescence counted were 9 inflorescences/m, that number is suggest at error, because, when it was compared with the final yield, the number of inflorescence was lower than bunches as show the figure 18. The mistake, in that case, was that the counting of inflorescence was late and not at well time, and due at high number of leaves, sometime the inflorescence were behind the leave making it difficult to count these. The highest number of inflorescences/m (12) was observed in SP4. The lowest number of inflorescences/m was observed on SP2 (8).

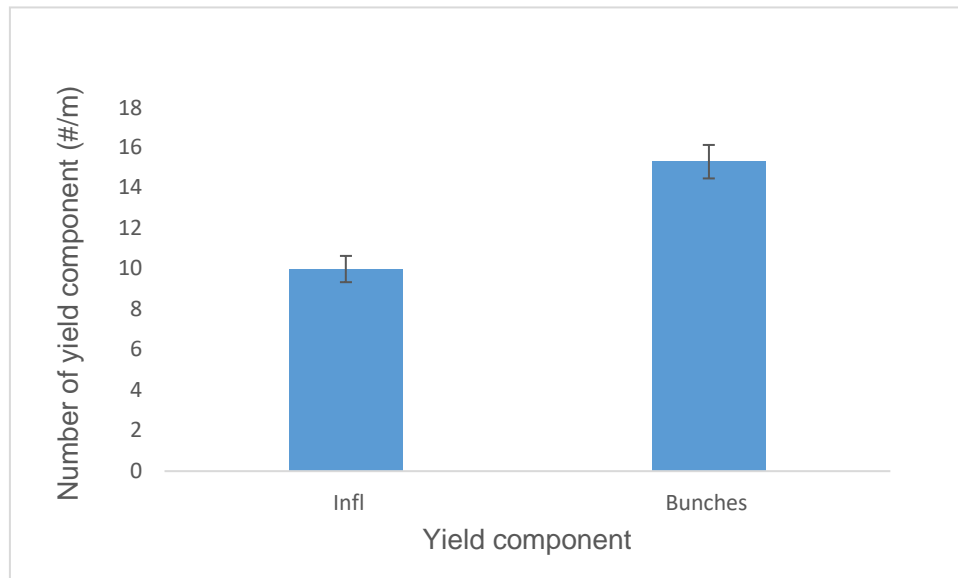


Figure 18. Number of inflorescences and number of bunches at harvest (#/m), and \pm standard error.

At pea-size it was counted the number of bunches, it was 15 bunch/m, it was assumed that the number of bunches will remain constant until harvest, because no cultural operation were planned as cluster thinning. The average of bunches per meter observed at pea-size and maturation is showed in table 3. The highest number of bunches was observed on SP4, as 185 bunches number, the lowest was on SP2, showing 121 bunches number. These difference of number of bunches, was because on the first row, as SP1 was subject a water stress and lower vigour.

Table 3. Number of bunches/m counted at pea-size and maturation.

Bunches at pea size (#/m)	Bunches at maturation (#/m)	Total bunches
15	15	699

The yield components previously counted on the vineyard were compared with the images from the VINBOT. When analysing the coefficient of correlation, the highest values were found at the stage of 4 leaves and maturation, showing $r=0.59$ and $r=0.64$ respectively (Fig. 19). The lower values observed at pea-size and veraison have occurred by due to the high vegetation cover, making the visibility of the respective yield components very difficult. This is confirmed in the visible inflorescence stage, where the comparison between the real observations and those in the images were found inconclusive. While at the stage of 4 leaves it was easy to

count the shoots, because for the presence of leaves, that they could help to distinguish the number of shoot in the images.

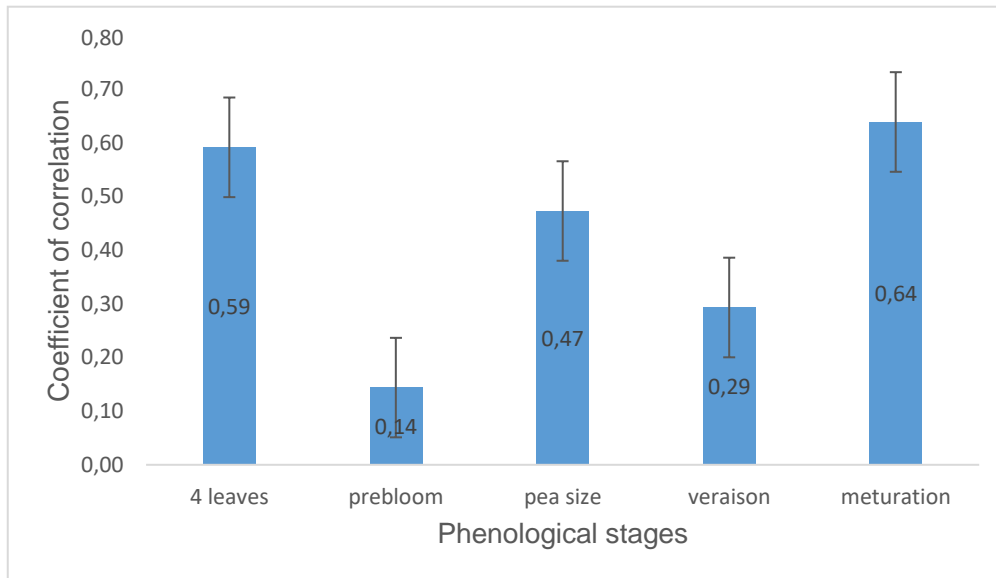


Figure 19. Coefficient of correlation and standard error observed between the images and ground truth, \pm standard error.

Table 4 show the coefficient of correlation between the MA%E and coefficient of correlation for each phenological stages. The highest error was found on the pea-size (73%), that error depended because the bunches not was well developed to be detected. At maturation was found the lower error (39%), because the vegetation allowed to detected the bunches.

Table 4. Relationship between % correlation coefficient and MA%E.

Stage	Correlation coefficient	MA%E
4 leaves	0.59	38%
prebloom	0.14	55%
pea size	0.47	73%
veraison	0.29	61%
maturation	0.64	39%

4.2 Projected area of bunch and weight

The relationship between the area of bunch (cm^2) and the weight of the bunch (g), show the coefficients of determinations (R^2) different for each phenological stage. These value of R^2 , was at pea-size 0.59 (Fig. 20), at veraison 0.61 (Fig. 21) and at maturation 0.90 (Fig. 22). The linear regression analysis, showed results highly significant for the three observed phenological stages. As showed from the linear regression analysis in figure 21, the projected area of bunches was able to explain ca 90% of bunches weight variability, indicating, as showed in Lopes *et al.*, (2016), that it can be uses as an accurate estimator for the weight of bunches.

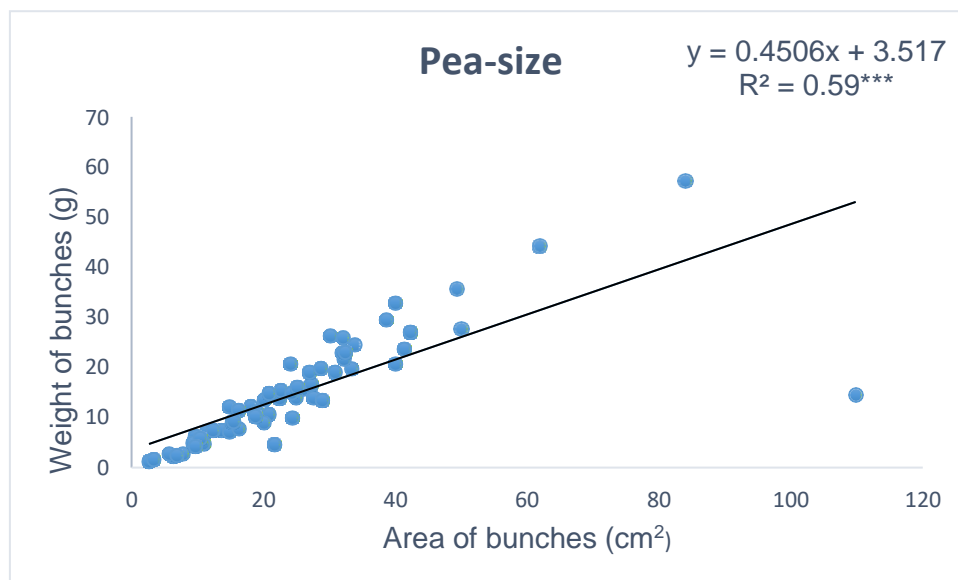


Figure 20. Relationship between area of bunches (cm^2) (variable independent) and bunches weight (variable dependent), linear regression equations and coefficient R^2 , at pea-size stage, $n= 60$. The * indicates the significant R^2 ($p \leq 0.001$).

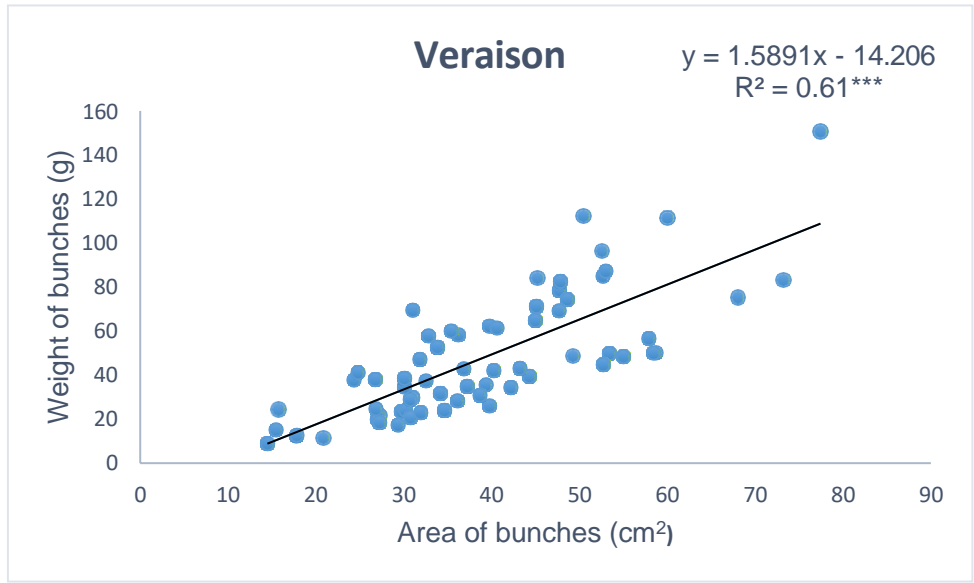


Figure 21. Relationship between area of bunches (cm²) (variable independent) and bunches weight (variable dependent), linear regression equations and coefficient R², at veraison stage, n= 60. The *** indicates the significant R² (p≤0.001).

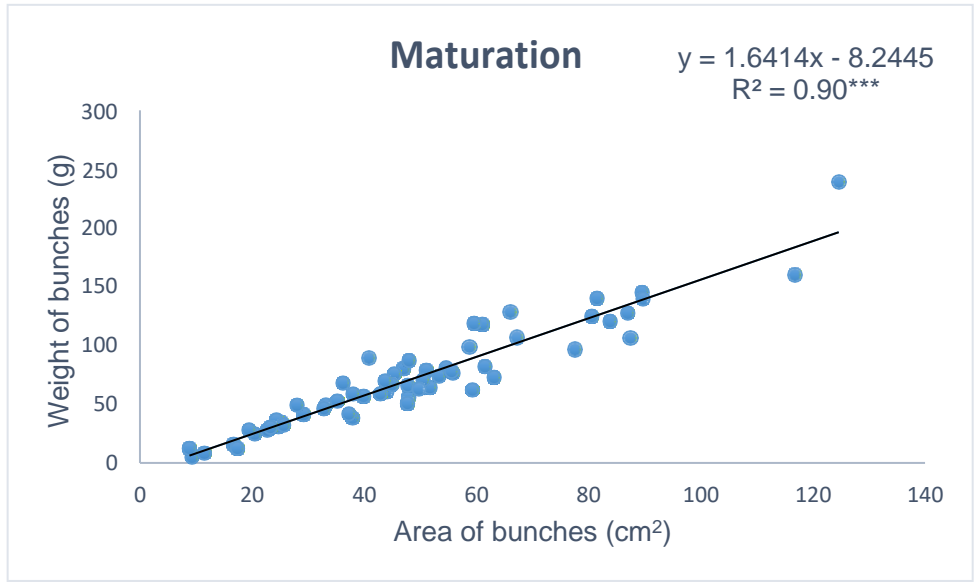


Figure 22. Relationship between area of bunches (cm²) (variable independent) and bunches weight (variable dependent), linear regression equations and coefficient R², at maturation stage, n= 60. The *** indicates the significant R² (p≤0.001).

4.3 Model for bunch estimation covered by leaves

For each phenological stages the percentage of bunches covered by leaves was 65% at pea-size, 69% at veraison and 47% at maturation. These values means that not all bunches are visible, because covered by leaves. The higher percentage of visible bunches was at maturation 53% of area of visible bunches. The higher % of visible bunches at maturation occurred because the climate condition in summer, as heat waves, determined sun burn of leaves, making the possibility to see more bunches. When it was calculated, the relationship between the porosity and area of visible bunches, at different level of defoliation showed a coefficient of determination for each phenological stages, as $R^2= 0.85$ at pea-pea size (Fig. 23), $R^2= 0.91$ (Fig. 24) at veraison and $R^2= 0.76$ at maturation (Fig. 25). These regression analysis, showed the coefficient of determination highly significant for each stages. As shown on a work of Lopes *et al.*, (2016), the significant R^2 indicating that the model can be used to estimate bunches covered by leaves. The values showed that increasing defoliation has been caused an increase of percentage of porosity, therefore the percentage of visible bunches was greater at high porosity.

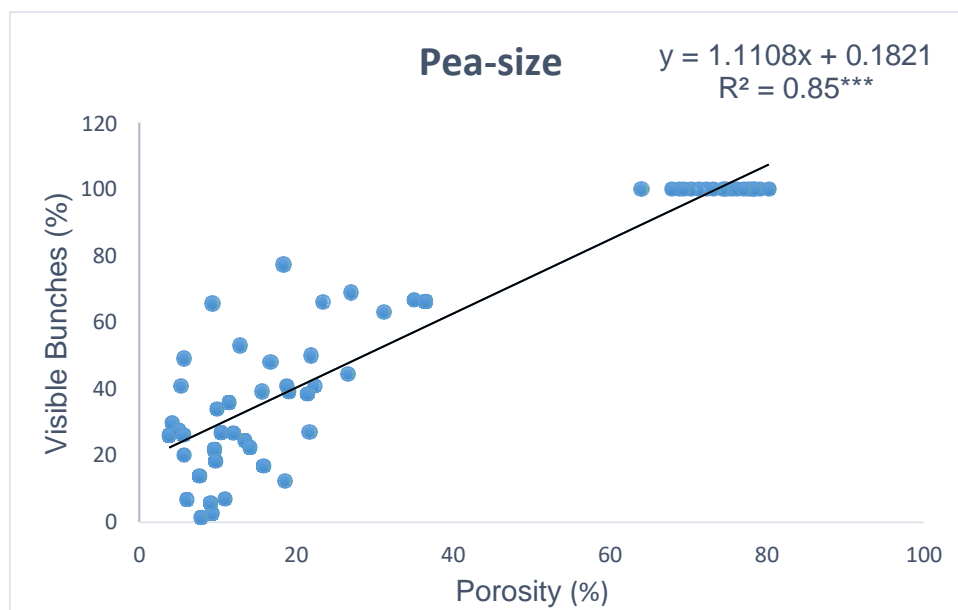


Figure 23. Relationship between % of porosity (variable independent) and % of visible bunches (variable dependent), showing the coefficient of determination (R^2) and regression equation, $n=20$. The *** indicates the significant R^2 ($p \leq 0.001$).

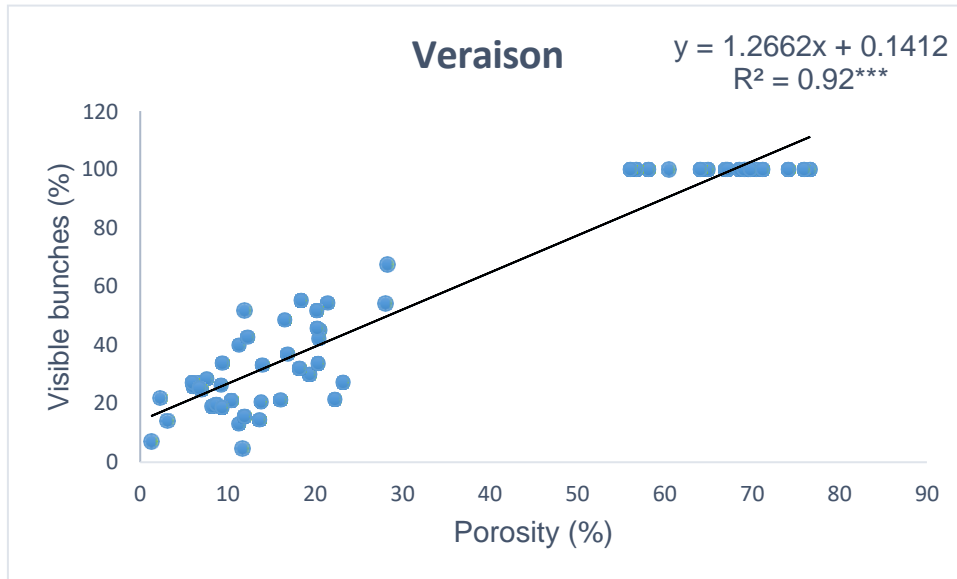


Figure 24. Relationship between % of porosity (variable independent) and % of visible bunches (variable dependent), showing the coefficient of determination (R^2) and regression equation, $n=20$. The *** indicates the significant R^2 ($p \leq 0.001$).

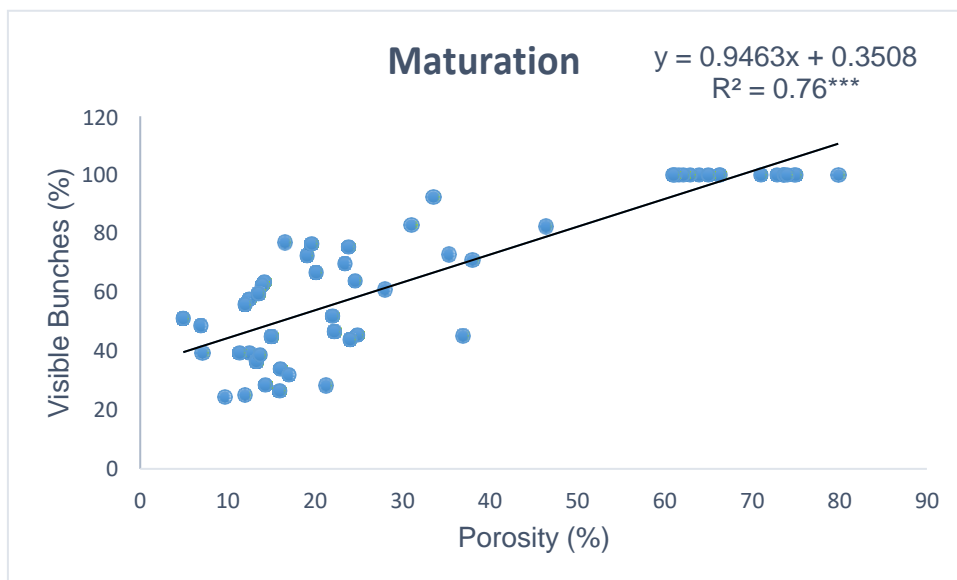


Figure 25. Relationship between % of porosity (variable independent) and % of visible bunches (variable dependent), with coefficient of determination (R^2) and regression equation, $n=20$. The *** indicates the significant R^2 ($p \leq 0.001$).

4.4 Model of bunch occlusion by other bunches

The table 5 shows the total occlusion of bunches by other bunches for each phenological stages. At pea-size and at veraison, the highest percentage of bunches occluded by others bunches, occurred in SP1 (52% at pea-size and 81% at veraison). At maturation the highest occlusion was found on SP3 (53%). The average of occlusion per meter was 6% at pea-size,

10% at veraison and 8% at maturity. Adding these values to the values of bunches covered by leaves (chapter 4.3), the percentage of visible bunches without these occlusion, by leaves and by others bunches, was 29% at pea size, 21% at veraison and 45 % at maturation. These percentages of visible bunches, in addition as explained above (chapter 4.3), are depended also of shapes of bunches. In our work occurred that some bunches were loses, however, the percentage of visible bunches was high.

Table 5. Average of occlusion per meter on each phenological stages.

Phenological Stage	Average occlusion per meter
Pea-size	6%
Veraison	10%
Maturation	8%

At maturation, the occlusion was lower at veraison, because at that stage, some berries were dried by heat waves occurred during the summer.

4.5 Berry and bunch growth factor

The average area of berries (Tab. 6) was at pea size 0.47 cm², at veraison was 1.73 cm² and at maturation was 1.29 cm². Between pea-size and veraison, the development of berries show a berries growth factor of 2.5. Between veraison and maturation, the development have almost stopped, the berries growth factor was 1.09. This low value was during growing phase, the availability of water was lower and the vines were suggested at water stress, also because they weren't irrigated (Dokoozlian, 2000)

Table 6. Average area of berries (cm²), the average area of bunches (cm²), the average weight (g) of bunches at maturation, and the growth factors between the phenological stages.

Phenologica l stage	Area Av. Berries (cm²)	Berry Growt h Factor	Area Av.bunches	Bunche s growth factor	Av. Bunches (g)	Bunches growth factor at maturity
Pea-size	0.47±0.15	2.5	25.13±17.95	1.55	14.84±10.56	4.85
Veraison	1.17±0.44	1.09	39.10±13.71	1.25	47.92±27.98	1.5
Maturation	1.29±25		48.10±24.7		72.06±42.82	

Regarding the average area per berries, as showed in the figure 26, the development of berries was slow between veraison and maturation. At maturation the berries were 2.7 times more developed as compared to pea-size.

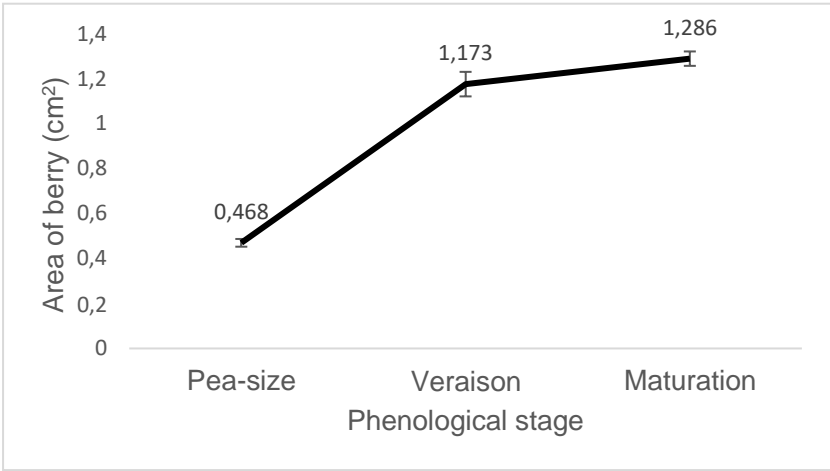


Figure 26. Evolution of average area of berries (cm²) for each phenological stages, the I represents the standard error.

As showed in the figure 27, the growth rate of the bunches was almost similar on the two periods considered (pea-size to veraison, and veraison to maturation).

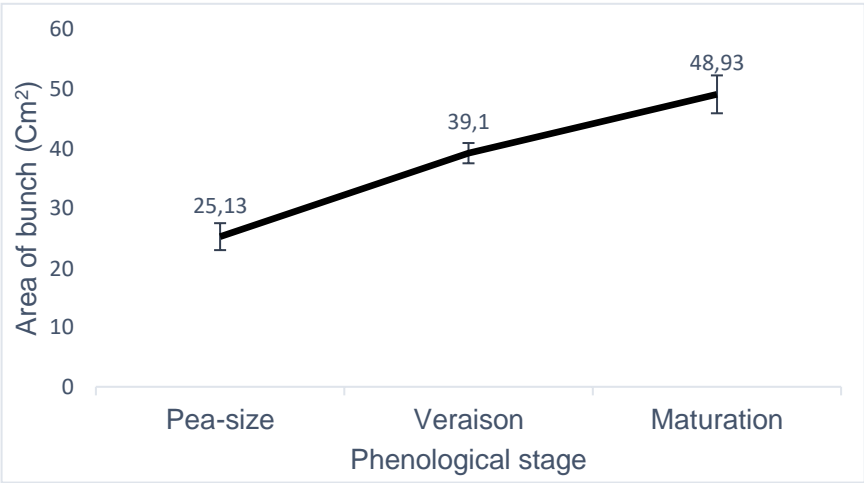


Figure 27. Evolution average area of bunch (cm²) for each phenological stages, the I represents the standard error.

Regarding the bunch growth factor, as show in the table 7, from pea-size to veraison was higher and then veraison to maturity. At maturation, bunches were 4.85 times more developed as compared to pea size.

Table 7. Values of bunch weight (g) and area (cm²), at three phenological stages.

	Pea-size	Veraison	Maturation
Area (cm ² /bunch)	25.13	39.10	48.93
Weight (g/bunch)	14.84	47.92	72.07

4.6 Final yield estimation

At harvest, it was observed the real yield of 0.81 kg/m. The real yield was compared with the yield estimated for each phenological stage. These values of yield, real and estimated, are shown in figure 28. As said in the chapter 3.5, the VINBOT cameras were used to estimate the porosity and visible area of bunches from pea-size to maturation. The table 7 shows the values of porosity and visible bunches. The highest percentage of porosity and visible bunches was obtained at maturation, which occurred for the same reason explained on the chapter 4.4. To estimate the yield it was used the real values per meter (not average) of porosity and area of visible bunches estimated by VINBOT cameras.

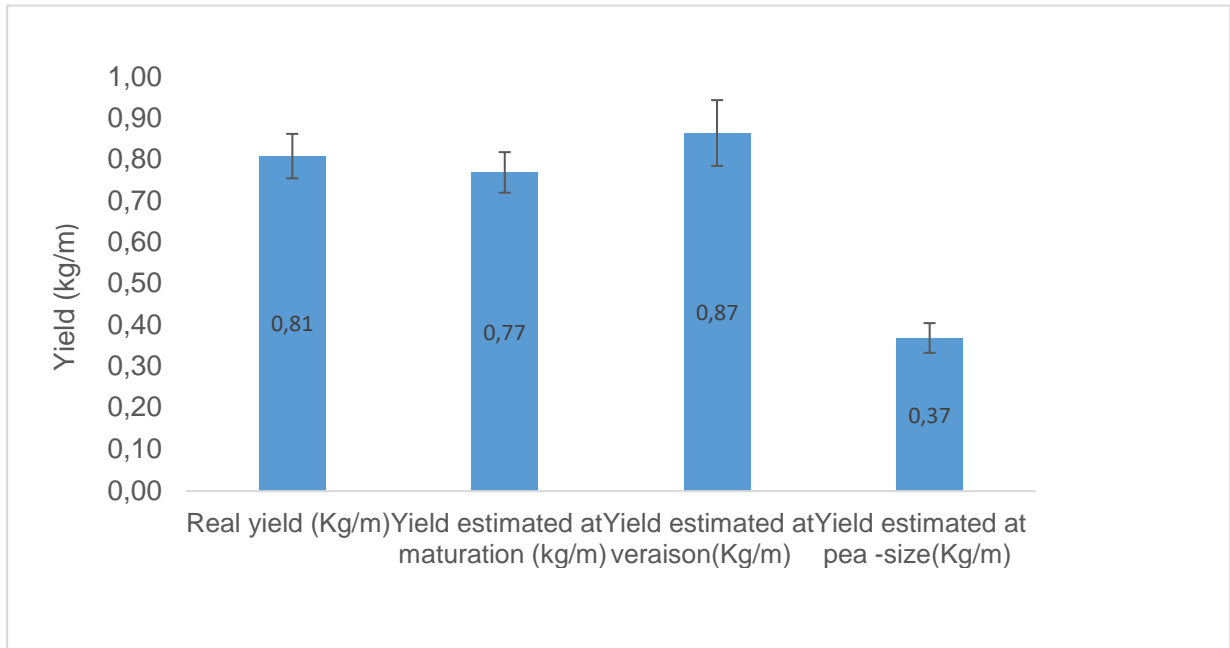


Figure 28. Average of yields (kg/m) using the camera RGB-d Kneticv2 of VINBOT.

Table 8. Average of porosity (%) and average of visible bunches (cm²), ± standard error.

Ph. Stages	Av. of porosity (%)	Av. Area of visible bunches (cm ²)
Pea-size	10±0.5	80.57±0.27
Veraison	12±0.44	130.44±0.81
Maturation	16±0.48	222.11±0.37

To estimate the yields, from pea-size to maturation, by adding the formulas from linear regression analysis (Tab. 9) obtained by the models estimated in the chapters 4.2, 4.3, and using the average of occlusion by bunches (chapter 4.4), and using the growth factors (chapter 4.5), it was possible to estimate the final yield (Fig. 29).

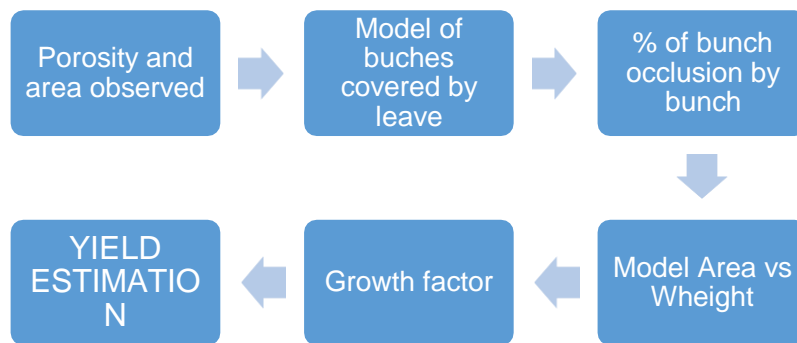


Figure 29. Flow chart for yield estimation, for each phenological stage.

Table 9. Formulas used for the yield estimation, for each phenological stage.

Model of area of bunches vs bunches weight		Equation	R²
	Pea size	$y=0.4506x+3.517$	0.59***
	Veraison	$y=1.5891x-14.206$	0.61***
	Maturation	$y=1.6414x-8.2445$	0.90***
Model of bunch covered by leaves			
	Pea-size	$y=1.1108x+0.1821$	0.85***
	Veraison	$y=1.226x+0.1412$	0.92***
	Maturation	$y=0.9463x+0.3508$	0.76***

Regarding the percentage of bunches occluded by other bunches, it was used at pea-size an occlusion of 6%, at veraison 10 % and at maturation 8%. The bunch growth factors used were 2.74 at pea-size and 1.09 at veraison.

As indicated in table 10, the model developed for yield estimation showed results very close to observed yield at veraison and at maturation, having an MA%E of 7% and 5%, respectively. At pea-size it was found the highest MA%E (54%).

Table 10. Relationship between the yield estimated and real yield, for each phenological stages, using the absolute error, percent mean absolute error.

		Estimate (kg/m)	Real (kg/m)	MAE (kg/m)	MA%E (%)
Pea-size	Yield kg/m	0.37	0.81	0.44	54
Veraison	Yield kg/m	0.87	0.81	0.5	7
Maturation	Yield kg/m	0.77	0.81	0.4	5

The statistics measures of validation (Table 9) showed that at pea-size an highest MAE and MA%E above the limits of acceptability suggested by Kleijnen (1987) ($\leq 10\%$) while at veraison and maturation within the limits. The results obtained from yield estimation show an underestimation at pea-size (0.37 kg/m) and at maturation (0.77 kg/m), while at veraison has been noted an overestimation (0.87 kg/m).

The comparison between real and estimated yield values using the data on each meters, for the three phenologicals stages, are presented in the figure 20. As show the figure 30A, at pea.size, it was underestimated the yield in almost all the meters, the meters that was

overestimated were 3, 19, 22, 23, 24, 25. While at veraison (Fig. 30B) and at maturation (Fig. 30C) had meters overestimated and underestimated.

Comparing the results obtained of this study with other yield estimation studies with different algorithm, this method can be catalogued as a great accurate one. As demonstrated yield estimation by Nuske *et al.*, (2014), it produced an average error between 3% and 11% of total yield.

As showed by Lopes *et al.*, (2016), the underestimation and overestimation of yield may be explained by bunch occluded by other bunch. The occlusion depend on bunch number per vine and bunch size. In this work is noticed variability in term of bunch size along the meters, this phenomenon may explained the underestimated and overestimated of yield.

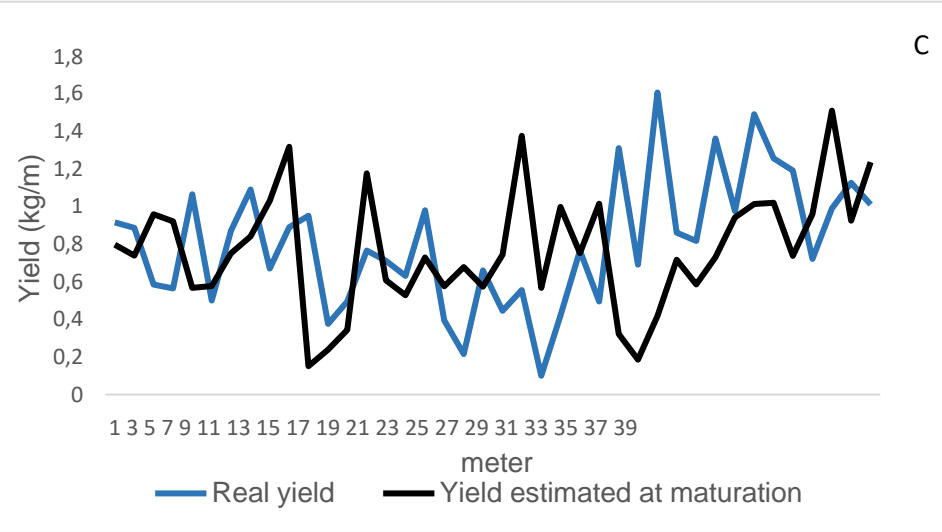
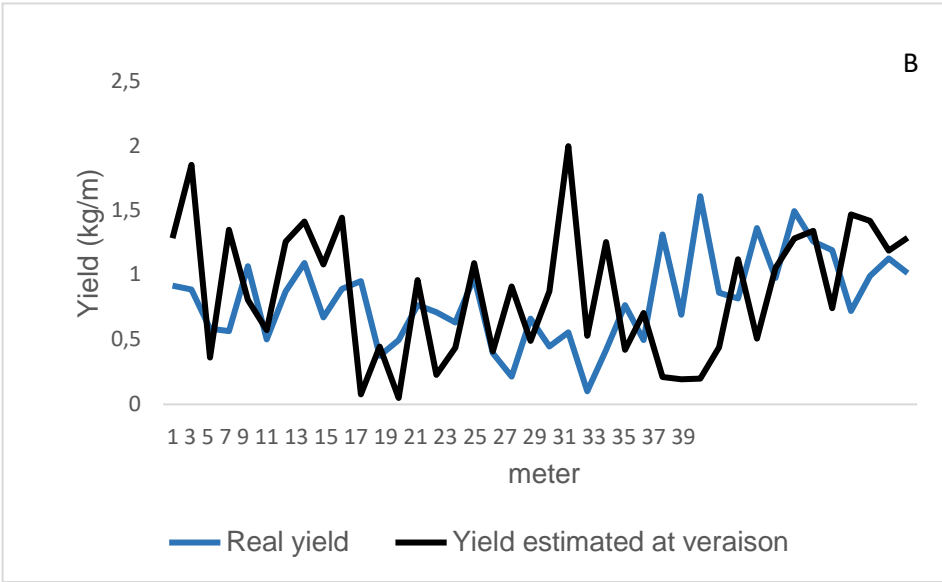
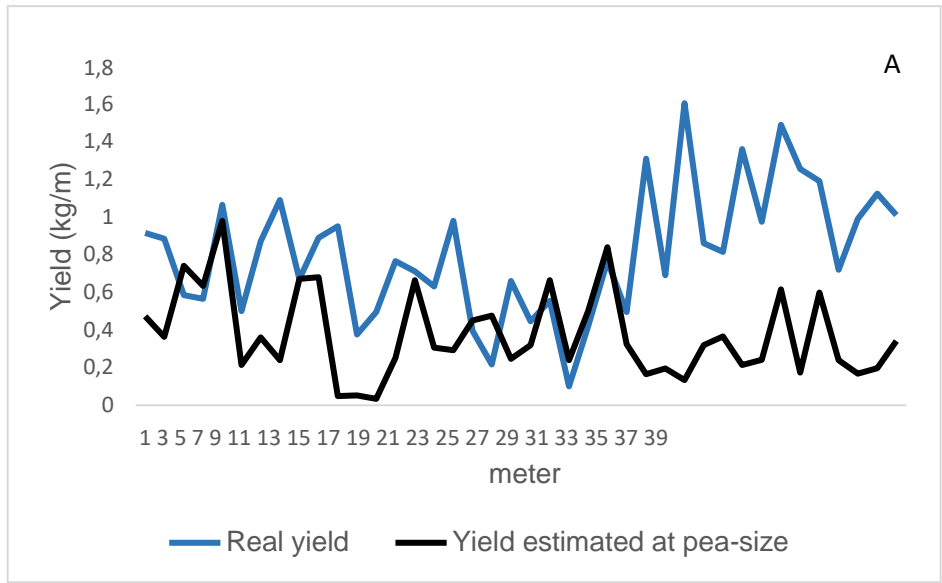


Figure 30. Real and estimated values of yield per meter, $n=40$. The (A) indicate pea-size, (B) indicate veraison and (C) maturation

5. CONCLUSIONS

The aims of this work were to collect data through the VINBOT robot to estimate the yield at early stages and near harvest of grapevine development and to contribute for the development of the VINBOT platform as a whole by improving its automatic yield estimation algorithms.

To estimate the final yield it were used models for non-visible bunches, and bunch growth factor. All the models were developed in this work. During the growing season 2019 were analysed the correlation between the ground truth and the data observed in the images.

The results showed a high correlation between the ground and the observation through images, indicating that the number of bunches can be use as variable to estimate the yield at pea-size.

The regression analysis between the projected area of bunches and bunch weight showed the highest coefficient of determination at maturation ($R^2= 0.90$), indicating that the projected area of bunches can be used as an accurate estimator for bunch weight.

The relationship between canopy porosity and exposed bunches showed for all the stages high and significant R^2 ($R^2 \geq 0.76$) indicating that we can use it to estimate bunches covered by leaves through image analysis.

In this work, it was noticed that the average percentage of occlusion of bunch by other bunch per meter was 6% at pea size, 10% at veraison and 8% at maturation. Adding the values of occlusion by leaves to these occlusion by bunches, the percentage of visible bunch was 29% at pea-size, 21% at veraison and 45% at maturation.

To estimate the yield at early stage, as pea-size or veraison, it was required the knowledge of bunch growth until maturation. Bunches, at maturation, were 4.85 times more developed as compared to pea-size stage. About the berry growth factor, it was low (1.09) from veraison to maturation, because during the growing phase, the vines were suggested at water stress.

About the final yield estimation, it was observed a small MA%E at veraison (7%) and maturation (5%), while at pea-size was 54%. In the yield estimation it was observed an underestimation at pea-size and maturation, and an overestimation at veraison, which can be attributed to bunch occlusion.

Considering the experimental conditions of this study, it is possible to conclude that the image analysis is an alternative to the traditional way to estimate the yield and the spatial variability in the vineyard.

Future Perspectives

During the season, different problems occurred, as the difficulty to analyse data in a specific phenological stage (i.e. flowering), because the VINBOT camera could not distinguish some vegetative components. To improve the quality of the images it should be used a new camera with better resolution, or reduce the distance between the row and VINBOT cameras.

The robot was used manually, it occurred that the distance between Robot and vines was different, determining that during the analysis of images, the scale of images was variable, increasing the error.

REFERENCES

- Al-Otum, H.M. (2003). Morphological operators for color image processing based on mahalanobis distance measure. *Optical Engineering*, 42, 2595–2606.
- Antcliff, A.J., May, P., Webster, W.J., Hawkes, J. (1972). The Merbein bunch count, a method to analyse the performance of grapevines. *American Society for Horticultural Science* 7(2), 196–197.
- Aquino, A., Millan, B., Gutiérrez, S., Tardáguila, J. (2015). Grapevine flower estimation by applying artificial vision techniques on images with uncontrolled scene and multi-model analysis. *Computers and Electronics in Agriculture*, 119, 92–104.
- Aquino, A., Diago, M. P., Millán, B., and Tardáguila, J. (2017). A new methodology for estimating the grapevine-berry number per cluster using image analysis. *Biosystems engineering*, 156, 80–95.
- Austin, C.N., Gove, G.G., Meyers, J.M., Wilcox, W.F. (2011). Powdery mildew severity as a function of canopy density: Associated impacts on sunlight penetration and spray coverage. *American Journal of Enology and Viticulture*, 62:23–31.
- Behroozi-Khazaei, N., Maleki, M.R. (2017). A robust algorithm based on color features for grape cluster segmentation. *Computers and electronics in agriculture*, 142, 41–49.
- Besselat, B., Cour, P. (1996). Early crop prediction. Summary and prospects for the use of a new tool based on pollen analysis of the atmosphere. In *Proceedings of the Agrometeorological Models: Theory and Applications in the Mars Project*. J. Dallemand and P. Vossen. Official Publications of the European Communities. ECSC-EAEC, Ispra, Italy, 73–82.
- Blom, P.E., Tarara, J.M. (2009). Trellis tension monitoring improves yield estimation in vineyards. *American Society for Horticultural Science*, 44(3), 678–685.
- Borgogno-Mondino, E., Lessio, A., Tarricone, L., Novello, V., de Palma, L. (2018). A comparison between multispectral aerial and satellite imagery in precision viticulture. *Precision agriculture*, 19(2), 195–217.
- Bubola, M., Peršurić, Đ., Kovačević Ganić, K., Karoglan, M., Kozina, B. (2012). Effects of fruit zone leaf removal on the concentrations of phenolic and organic acids in Istrian Malvasia grape juice and wine. *Food Technology and Biotechnology*, 50:159–166.

Cerovic, Z.G., Moise, N., Agati, G., Latouche, G., Ben Ghazlen, N., Meyer, S. (2008). New portable optical sensors for the assessment of winegrape phenolic maturity based on berry fluorescence. *Journal of Food Composition and Analysis*, 21:650–654.

Clingeffer, P.R., Martin, S.R., Dunn, G.M., Krstic, M.P. (2001). Crop development, crop estimation and crop control to secure quality and production of major wine grape varieties: a national approach: final report to Grape and Wine Research & Development Corporation/principal investigator, Peter Clingeffer; [prepared and edited by Steve Martin and Gregory Dunn].

Connolly, C., Fleiss, T. (1997). A study of efficiency and accuracy in the transformation from RGB to CIELAB colour space. *IEEE Transactions on Image Processing*, 6 (7), 1046-1048.

Cour, P. (1974). Nouvelles techniques de détection des flux et des retombées polliniques: Etude de la sédimentation des pollens et des spores à la surface du sol. *Pollens Spores*, 16(1):103–141.

Cousin, I., Besson, A., Bourennane, H., Pasquier, C., Nicoullaud, B., King, D., Richard, G. (2009). From spatial-continuous electrical resistivity measurements to the soil hydraulic functioning at the field scale. *Comptes Rendus Geoscience*, 341:859–867.

Cristofolini, F., Gottardini, E. (2000). Concentration of airborne pollen of *Vitisvinifera* L. and yield forecast: a case study at S. Michele all'Adige, Trento, Italy. *Aerobiologia*, 16(1), 125–129.

Crookston, R.K. (2006). A top 10 list of developments and issue impacting crop management and ecology during the past 50years. *Crop Science*, 46(5), 2253–2262.

Cubero, S., Diago, M.P., Blasco, J., Tardáguila, J., Prats-Montalbán, J.M., Ibáñez, J., Tello, J., Aleixos, N. (2015). A new method for assessment of bunch compactness using automated image analysis. *Australian Journal of Grape and Wine Research*, 21, 101-e109.

Cunha, M., Abreu, I., Pinto, P., Castro, R. (2003). Airborne pollen samples for early-season estimates of wine production in a mediterranean climate of northern Portugal. *American Journal of Enology and Viticulture*, 54, 189–194.

Cunha, M., Marcal, A.R., Silva, L. (2010). Very early prediction of wine yield based on satellite data from vegetation. *International Journal of Remote Sensing*, 31(12), 3125–3142.

Diago, M.P., Correa, C., Millán, B., Barreiro, P., Valero, C., Tardáguila, J. (2012a). Grapevine yield and leaf area estimation using supervised classification methodology on RGB images taken under field conditions. *Sensors*, 12(12), 16988–17006.

- Diago, M.P., Krasnow, M., Bubola, M., Millan, B., Tardáguila, J. (2016). Assessment of vineyard canopy porosity using machine vision. *American Journal of Enology and Viticulture*, 67(2), 229–238.
- Diago, M.P., Sanz-Garcia, A., Millan, B., Blasco, J., Tardáguila, J. (2014). Assessment of flower number per inflorescence in grapevine by image analysis under field conditions. *Journal of the Science of Food and Agriculture*, 94(10), 1981–1987.
- Diago, M.P., Tardáguila, J., Aleixos, N., Millan, B., Prats-Montalban, J.M., Cubero, S., Blasco, J. (2015). Assessment of cluster yield components by image analysis. *Journal of the Science of Food and Agriculture*, 95(6), 1274–1282.
- Diago, M.P., Ayestarán, B., Guadalupe, Z., Poni, S., Tardáguila, J. (2012b). Impact of pre-bloom and fruit-set basal leaf removal on the flavonol and anthocyanin composition of Tempranillo grapes. *American Journal of Enology and Viticulture*, 63:367–376.
- Diago, M.P., Vilanova, M., Tardáguila J. (2010). Effects of timing of manual and mechanical early defoliation on the aroma of *Vitis vinifera* (L.) Tempranillo Wine. *American Journal of Enology and Viticulture*, 61:382–391.
- Dobrowski, S.Z., Ustin, S.L., Wolpert, J.A. (2003). Grapevine dormant pruning weight prediction using remotely sensed data. *Australian Journal of Grape and Wine Research* 9, 177–182.
- Dokoozlian, N.K. (2000). Grape berry growth and development. *Raisin production manual*, 3393, 30.
- Dunn, G.M. (2010). Yield forecasting. Technical Booklet. University of Melbourne, Australia, Grape and Wine Research and Development Corporation.
- Dunn, G.M., Martin, S.R. (2004). Yield prediction from digital image analysis: A technique with potential for vineyard assessments prior to harvest. *Australian Journal of Grape and Wine Research*, 10(3), 196–198.
- Dunn, G.M., Martin, S.R. (2007). A functional association in *Vitis vinifera* L. cv. Cabernet Sauvignon between the extent of primary branching and the number of flowers formed per inflorescence. *Australian Journal of Grape and Wine Research*, 13(2), 95–100.
- Fregoni, M. (1999). *Viticultura di qualità*. L'informatore agrario. VII, 127-213.
- Gebbers, R., Adamchuk, V.I. (2010). Precision agriculture and food security. *Nature*, 327, 828–831.

- Gitelson, A.A., Kaufman, Y.J., Stark, R., Rundquist, D. (2002). Novel Algorithms for Remote Estimation of Vegetation Fraction, *Remote Sensing of the Environment*, 80, 76–87.
- Gommes, R. (1998). Agrometeorological crop yield forecasting methods. *International Conference of Agricultural Statistics*, 11.
- Grossetete, M., Berthoumieu, Y., Da Costa, J.P., Germain, C., Lavialle, O., Grenier, G. (2012). Early estimation of vineyard yield: site specific counting of berries by using a smartphone. *International Conference of Agricultural Engineering—CIGR-AgEng*.
- Hall, A., Lamb, D.W., Holzapfel, B., Louis, J. (2002). Optical remote sensing applications in viticulture – a review. *Australian Journal of Grape and Wine Research*, 8:36–47.
- Herrero-Huerta, M., González-Aguilera, D., Rodríguez-Gonzálvez, P., Hernández-López, D. (2015). Vineyard yield estimation by automatic 3D bunch modelling in field conditions. *Computers and electronics in agriculture*, 110, 17–26.
- Hunt, E.R., Doraiswamy, P.C., McMurtrey, J.E., Daughtry, C.S.T., Perry, E.M., (2013). A Visible Band Index for Remote Sensing Leaf Chlorophyll Content at the Canopy Scale, *International Journal of Applied Earth Observation and Geoinformation*, 21, 103–112.
- Jones, G.H., Vaughan, R.A. (2010). *Remote sensing of vegetation*. Oxford, 95–96, 100.
- Kleijnen, J.P.C. (1987). *Statistical tools for simulation modeling and analysis*. McGraw-Hill, New York.
- Komm, B., Moyer, M. (2015). *Vineyard yield estimation*. Washington State University.
- Krizhevsky, A., Sutskever, I., Geoffrey, E.H. (2012). ImageNet Classification with Deep Convolutional Neural Networks. *Advances in Neural Information Processing Systems*, 25, 1097–1105.
- Liu, S., Cossell, S., Tang, J., Dunn, G., Whitty, M. (2017). A computer vision system for early stage grape yield estimation based on shoot detection. *Computers and Electronics in Agriculture*, 137, 88–101.
- Lopes, C.M., Torres, A., Guzman, R., Graça, J., Reyes, M., Vitorino, G., Barriguiha, A. (2016). Using an unmanned ground vehicle to scout vineyards for non-intrusive estimation of canopy features and grape yield.
- Loy, G., Zelinsky, A. (2003). Fast radial symmetry for detecting points of interest. *IEEE Transactions on Pattern Analysis and Machine Intelligence*, 25, 959–973.

Martin, S., Dunstone, R., Dunn, G. (2003). How to forecast wine grape deliveries using grape forecaster excel workbook version 7. Australian Grape and Wine Research and Development Corporation, Adelaide, Australia, 100.

Matese, A., Di Gennaro, S.F. (2015). Technology in precision viticulture: A state of the art review. *International Journal of Wine Research*, 7, 69–81.

Matheron, G. (1975). *Random Sets and Integral Geometry*, Wiley, New York, NY, USA.

McBratney, A., Minasny, B., Whelan, B. (2011). Defining proximal soil sensing. In: IUSS, editor. *Second global workshop on proximal soil sensing*. Montreal: IUSS Working Group on Proximal Soil Sensing, 144–146.

Millan, B., Aquino, A., Diago, M.P., Tardaguila, J. (2017). Image analysis-based modelling for flower number estimation in grapevine. *Journal of the Science of Food and Agriculture*, 97(3), 784–792.

Monteiro, A., Teixeira, G., Santos, C., & Lopes, C. M. (2018). Leaf morphoanatomy of four red grapevine cultivars grown under the same terroir. In *E3S Web of Conferences*. EDP Sciences.

Nobuyuki, O. (1979). A threshold selection method from graylevel histograms. *IEEE Transactions on Systems, Man and Cybernetics*, 9, 62e66.

Nuske, S., Achar, S., Bates, T., Narasimhan, S., Singh, S. (2011). Yield estimation in vineyards by visual grape detection. In *2011 IEEE/RSJ International Conference on Intelligent Robots and Systems*, San Francisco, CA, USA, 2352–2358.

Nuske, S., Wilshusen, K., Achar, S., Yoder, L., Narasimhan, S., Singh, S. (2014). Automated visual yield estimation in vineyards. *Journal of Field Robotics*, 31(5), 837–860.

Palliotti, A., Silvestroni, O. (2004). *Ecofisiologia applicata alla vite*. In: *Viticultura ed enologia biologica*. Eugenio Cozzolino (ed), 41–88. Edagricole. Bologna, Italia.

Portal do Clima (2019). Portal do Clima website. (Portugal) <http://portaldoclima.pt/en/#>

Reynolds, A.G., Wardle, D.A. (1989). Influence of fruit microclimate on monoterpenes levels of Gewürztraminer. *American Journal of Enology and Viticulture*, 40:149–154.

Rossel, R.V., Minasny, B., Roudier, P., McBratney, A.B. (2006). Colour space models for soil science. *Geoderma*, 320–337.

Rudolph, R., Herzog, K., Töpfer, R., Steinhage, V. (2018). Efficient identification, localization and quantification of grapevine inflorescences in unprepared field images using fully convolutional networks.

- Santesteban, L.G. (2019). Precision viticulture and advanced analytics. A short review. *Food chemistry*, 279, 58–62.
- Serra, J. (1980). The Boolean model and random sets. *Computer Graphics and Image Processing*, 12(2) 99–126.
- Smart, R., Robinson, M. (1991). *Sunlight into the wine. A handbook for winegrape canopy management*. Winetitles, Adelaide.
- Smart, R., (1987). Influence of light on composition and quality of grapes. *Acta Horticulture*, 206:37–47.
- Son, J., Inoue, N., Yamashtia, Y. (2010). Geometrically local isotropic independence and numerical analysis of the mahalanobis metric in vector space. *Pattern Recognition Letters*, 31, 709–716.
- Spalding, E.P., Miller, N.D. (2013). Image analysis is driving a renaissance in growth measurement. *Current Opinion in Plant Biology*, 16(1), 100–104.
- Srinivasan, A. (2006). *Handbook of precision agriculture. Principles and applications*. New York; London; Oxford: Food Products Press.
- Tardáguila, J., Diago, M.P., Millan, B., Blasco, J., Cubero, S., Aleixos, N. (2012). Applications of computer vision techniques in viticulture to assess canopy features, cluster morphology and berry size. *International Workshop on Vineyard Mechanization and Grape and Wine Quality 978*, 77–84.
- Tardáguila, J., Herrero-Langreo, A., Barreiro, P., Valero, C., Poni, S., Diago, M.P. (2011). Using RGB image analysis to assess the impact of early defoliation on the fruit zone. *Proceedings of International Symposium GIESCO. Asti-Alba, Italy*.
- Tardáguila, J., Blanco J.A., Poni S., Diago, M.P. (2012). Mechanical yield regulation in winegrapes: Comparison of early defoliation and crop thinning. *Australian Journal of Grape and Wine Research*, 18:344–352.
- Taylor, J., Tisseyre, B., Bramley, R., Reid, A., Stafford, J. (2005). A comparison of the spatial variability of vineyard yield in European and Australian production systems. In *Precision agriculture'05. Papers presented at the 5th European Conference on Precision Agriculture*, Uppsala, Sweden, Wageningen Academic Publishers, 907–914.
- Vinbot (2019). Vinbot website. <http://vinbot.eu/robot-2/robot/>

Zarco-Tejada, P.J., Miller, J.R., Mohammed, G.H., Noland, T.L., Sampson, P.H. (2002).
Vegetation stress detection through chlorophyll a + b estimation and fluorescence effects on
hyperspectral imagery. *Journal of Environmental Quality*, 31(5):1433–1441.

APPENDIX

A.1 Analysis of yield component

The area was calculated using the software “imageJ”. The step to know the area is: **1** open the program and put the photo on it (only one meter was selection); **2** set the scale, open “*analyse*”, following “*set scale*”, open a window where in “*know distance*”, the correct value of the length of the line drawn on the scale of the photo is inserted and the units are positioned in cm; **3** select the image to work; **4** “press the button “*multiple selection*”, only the bunches must be selected; **5** click on ctrl+m, the result is the area of bunches. In the laboratory was performed the photos of measurement detailed of single bunches with the labels in two prospective. In these image was calculated the area of single bunches, the area is the mean of these two prospective. The calculation of the area was performed in this way: **1** open the program and put the photo on it (only one meter was selection); **2** set the scale, open “*analyse*”, following “*set scale*”, open a window where in “*know distance*”, the correct value of the length of the line drawn on the scale of the photo is inserted and the units are positioned in cm; **3** select the image, and in this image, push on “*adjust*” after “*colour threshold*”. Will open a window, where in “*colour space*” select RGB. The image becomes all embodied, adjust the colour to make red the green part; **4** click on “*select*” then “*analyse*”, the result is area of bunches.

A.2 Estimation of projected area of bunches in the images

The following steps were performed in ImageJ: **1** open the program and put the photo on it (only one meter was selection); **2** set the scale, open “*analyse*”, following “*set scale*”, open a window where in “*know distance*”, the correct value of the length of the line drawn on the scale of the photo is inserted and the units are positioned in cm; **3** select the image to work, select in the “Image” menu the option “Crop” then “Adjust” and “Colour Threshold”. Will open Threshold color panel where in “colour space”, select RGB and the colors Red, Blue and Green. The images is all red, adjust in blue so that the red curl appears, select “select” to appear the cluster of green color and with a yellow line delimiting it; **4**: in the menu “analyse” and “measure”. **5**: opens a “result” window indicating the area in cm².

A.3 Evaluation of porosity

The porosity was calculate in %, higher % of porosity higher is the % area of visible cluster. The protocol for the grapevine is described following. To evaluate the porosity is required the image analysis software, in that case we used “image J” and the grapevine RGB photographs

with a monochromatic background, in our case used a blue background, and a scale. The steps for analyse the image were: **1** open the program and put the photo on it (only one meter was selection); **2** set the scale, open “*analyse*”, following “*set scale*”, open a window where in “*know distance*”, the correct value of the length of the line drawn on the scale of the photo is inserted and the units are positioned in cm; **3** select the image, and in this image, push on “*adjust*” after “*colour threshold*”. Will open a window, where in “*colour space*” select RGB. The image becomes all embodied, adjust the colour to make red the blue part; **4** in this step need to assess both the area of the initial image, on the top of the image have two number, the multiplication of these number is the area, and the blue area, after “*colour threshold*”, click on “*select*” then “*analyse*”, the result is the blue area; **5** calculation of porosity %, is it Blue area/ Image Area.

A.4 Calculation of number of berries

The berries count was performed using the RGB images from a compact camera analysed with the software “ImageJ”. The calculation of berries was performed in this way: **1** open the image to be counted. If it is a colour image (RGB), it will have to be converted to grayscale before proceeding, click on “*image*”, “*type*” and convert in 8- or 16-bit.; **2** use the image, go on “*adjust*”, “*threshold*”, to highlight all of the structure to count, to do it click on “*set*”; **3** count the berries, go to “*analyze*”, “*analyze particle*”. There are some choices that can affect the counts from images. If need to remove these choices, when open “*analyze particle*”, need to changes the value on “*size*”, a values adjusted to the area of berries and different from 0 (e.i. 0.1-infinity), in “*show*”: select (Count) and OK. It open a window “*results*” with area indication in cm² of each berry, ad a window “*summary*” with indication of number of berries.



Departamento de Ciências e Engenharia de Biosistemas

PARECER

Na qualidade de orientador da dissertação de mestrado do aluno **Giuseppe Samà** intitulada **“Grapevine yield estimation using image analysis for the variety Syrah”**, confirmo que o aluno procedeu às alterações sugeridas pelos membros do júri.

Instituto Superior de Agronomia, 23 de Janeiro de 2020

Orientador

(Carlos M. A. Lopes; Prof. Associado)